UNIVERSITY OF CALIFORNIA, SAN DIEGO

Volcanic, Erosional, Tectonic, and Biogenic Peaks on Guyot Summit Plains in the Louisville Seamount Chain

A thesis submitted in partial satisfaction of the requirements for the degree

Master of Science

in

Earth Sciences

by

Daniel R. Ebuna

Committee in charge:

Professor Peter Lonsdale, Chair
Professor Steve Cande
Professor Pat Castillo
Professor Edward Winterer

2011

The Thesis of Daniel R. Ebuna is approved and it is acceptable in quality and form for publication on microfilm and electronically:

Chair

University of California, San Diego

2011

To my parents, Tim and Mary Ebuna

“The finest workers in stone are not copper or steel tools, but the gentle touches of air and water at their leisure with a liberal allowance of time.”

- Henry David Thoreau

TABLE OF CONTENTS

Signature Page..... iii

Dedication..... iv

Epigraph..... v

Table of Contents..... vi

List of Figures..... viii

Acknowledgements..... ix

Abstract..... xi

1 INTRODUCTION..... 1

1.1 Guyot Morphology..... 2

1.2 Previous Volcanic Island Morphology Studies..... 3

1.3 Regional Setting..... 8

2 DATA & METHODS..... 12

2.1 Multibeam Bathymetry Data..... 13

2.2 Multichannel Seismic Reflection Data..... 14

2.3 CHIRP – 3.5 kHz Knudsen Data..... 17

2.4 Dredge Samples..... 17

3 DISCUSSION..... 19

3.1 Bubble Pulse Multiples in MCS Data..... 20

3.2 Fluid Flow and Lithification of Guyot Surfaces..... 24

3.3 Multiple Origins of Louisville Guyot Peaks..... 26

3.3.1 Peaks of Constructional Volcanic Origin..... 26

3.3.2 Peaks of Erosional Origin..... 32

3.3.3 Louisville Guyots with Constructional and Erosional Peaks..... 37

3.3.4 Peaks of Tectonic Origin..... 41

3.3.5 Peaks of Biogenic Origin..... 44

3.3.6 Timing of Carbonate Reefs on Louisville Guyots..... 53

4 CONCLUSIONS..... 56

Appendix..... 63

References..... 74

LIST OF FIGURES

Figure 1: Sea-surface isotherms for the coldest month of the year..... 6

Figure 2: Regional map of the Louisville Seamount Chain..... 9

Figure 3: MCS Profile 27.6-6 displaying bubble pulse multiple..... 21

Figure 4: (a) Guyot 168.0°W reflectivity map..... 23

(b) Section of Profile 168.0-1 demonstrating reflectivity correlation..... 23

Figure 5: Section of Profile 168.0-8 with potential evidence of fluid flow..... 25

Figure 6: Bathymetry of constructional volcanic cones on Guyot 165.4°W..... 28

Figure 7: Bathymetry of Guyot 26.6°S showing potential transitional peaks..... 29

Figure 8: (a) MBedit display showing suspected erosional shelf on 26.6°S..... 31

(b) Fledermaus view of bathymetric data displaying transitional peaks... 31

Figure 9: Small-scale bathymetric map of erosional peaks on Guyot 27.6°S..... 34

Figure 10: MCS data from Guyot 27.6°S (small-scale view of Profile 27.6-4)..... 35

Figure 11: (a) Map of erosional remnant on the northern core of Guyot 169.0°W.... 39

(b) Map of volcanic cone on the southern core of Guyot 169.0°W..... 39

Figure 12: Constructional peak on Guyot 169.0°W as seen in MCS data..... 40

Figure 13: Bathymetric map of Guyot 26.0°S showing highly-faulted nature..... 43

Figure 14: Small-scale map of the carbonate platform on Guyot 168.0°W..... 45

Figure 15: MCS data displaying carbonate platform structure on Guyot 168.0°W... 47

Figure 16: Graph showing relative positions of guyots with peaks of each origin..... 58

ACKNOWLEDGEMENTS

First and foremost, I would like to thank my colleagues at Scripps Institution of Oceanography for making the past few years such an enjoyable learning experience. I would like to acknowledge my advisor Dr. Peter Lonsdale for bringing me in to the fascinating world of marine geomorphology and providing me the opportunity to gain oceanographic field experience. Through my research with him, I have learned a great deal about the collection and application of marine geophysical data. I especially wish to thank my fellow graduate student and officemate, Jared Kluesner, for his patience and expertise in teaching me the fine arts of shell scripting and multichannel seismic reflection data processing.

Secondly, I would like to thank the outside consultants who assisted Jared and me in refining our seismic data processing scheme. Antonio Gonzales of CICESE and a retired industry professional, Reginald Beardsley, were instrumental in teaching us not only how to perform the necessary processing steps, but also helping to provide a clear understanding of why each step is applied.

A big thank you also goes to the Integrated Ocean Drilling Program (IODP) and the co-chief scientist of Expedition 330, Dr. Anthony Koppers, for selecting me to take part in the recent drilling cruise to the Louisville Seamount Chain. This expedition provided great insight into ship-based drilling, international academic programs, and scientific writing by committee. The funding associated with this cruise was vital to my final year of research at Scripps.

Last but not least, I wish to thank my friends and family for all of the support and encouragement they have provided over the years. I am incredibly fortunate to have such loving parents who have given me the endless emotional and financial support that has helped me to reach this point in my academic career and in life.

ABSTRACT OF THE THESIS

Volcanic, Erosional, Tectonic, and Biogenic Peaks on
Guyot Summit Plains in the Louisville Seamount Chain

by

Daniel R. Ebuna
Master of Science in Earth Sciences
University of California, San Diego, 2011
Professor Peter Lonsdale, Chair

This study utilizes the geomorphology of guyots in the Louisville Seamount Chain to gain insight into the magmatic, erosional, and plate tectonic processes that have dominated the region. By studying the features that result from these complex processes, it becomes possible to hypothesize about how such edifices developed through time. While the majority of guyot studies have focused on the depth and nature of the transition from guyot summit plains to the flank slopes, this research takes advantage of high-resolution marine geophysical data to analyze the much smaller-scale features (peaks) that interrupt the otherwise flat guyot summit plains.

Multibeam bathymetry, multichannel seismic reflection profiles, 3.5 kHz profiles, and numerous dredge samples were collected during a 2006 site survey cruise to the Louisville Seamount Chain in the Southwest Pacific Ocean. All of these sources of geologic information were used in combination to make observations about the morphology and composition of the guyot summit plain peaks found in the chain. Then, by comparing these features with landforms already well-established in scientific literature, it becomes possible to postulate the specific origin of each individual peak. The four mechanisms of peak formation identified in this study are: constructional volcanic processes, erosional residuals, tectonic deformation, and biogenic carbonate-reef growth. The spatial and temporal relationships among these different origins of guyot summit plain peaks can then be evaluated in order to draw conclusions about the evolution of the seamount chain as a whole.

1

Introduction

1.1 GUYOT MORPHOLOGY

The geomorphology of hotspot guyots is considered by many investigators to possess a wealth of marine geologic information; by studying what processes are responsible for giving these edifices their final shapes, and also when, it becomes possible to make observations about the behavior of the system as a whole. Guyots were originally defined by Hess [1946] to be submarine, flat-topped peaks with steeply sloping sides, which he thought were suggestive of volcanic cones that had experienced wave truncation. This purely descriptive definition allows for submarine edifices with flat summits of any origin to be called guyots, without regard to the composition of the guyot summit plain or whether it was formed constructionally or erosionally. A more specific definition for guyots based on their genesis, and the one that shall be used here, is a volcanic edifice that developed a relatively flat top while at sea level due to a combination of littoral and subaerial erosion, then became submerged due to thermal subsidence of the underlying lithosphere.

Many of the flat, circular plan form edifices with low-sloping beveled edges that Hess had observed are the result of thick pelagic sediment beds having been trimmed by currents around the perimeter [Karig et al., 1970]. In other instances, the flat-topped features are formed primarily by carbonate reef growth, and therefore are not true guyots based on their constructional biogenic origin. These proto-atolls also often exhibit low-sloping beveled perimeters due to differential compaction of limestone units [Winterer et al., 1995]. So clearly, the morphologies of the observed surfaces are not actually representative of the state the edifices were in at the time of submergence. To study the nature of the actual summit plain, subsurface data is required, or the region of

interest needs to have had very low sediment supply and lack carbonate reefs. This investigation utilizes the best subsurface data coverage available for a major guyot chain. Additionally, these edifices were formed at high latitudes, unlike the majority of Pacific seamounts, which means they should be unaffected by tropical reef growth and the high pelagic sediment input associated with the equatorial upwelling region.

Many guyot summit plains have steep cones, ridges, or broad mounds built upon them. This study suggests that the origin of these peaks can be ascribed to one of four potential mechanisms using high-resolution geophysical data coverage and geological samples for groundtruthing. The four possible origins for summit plain peaks discussed in depth here are: constructional volcanic cones, erosional remnants, tectonic deformation, and biogenic reef growth. The correct identification of these features in guyot studies is of primary importance in understanding of the temporal and spatial relationships of the volcanic chain as a whole.

1.2 PREVIOUS VOLCANIC ISLAND MORPHOLOGY STUDIES

Many authors have investigated the geomorphological expression of oceanic islands from their inception to emergence and subsidence below sea level, and even through to subduction into a trench [Davies et al., 1972; Menard, 1984; Vogt and Smoot, 1984; Lonsdale, 1986, 1988; Barone and Ryan, 1987; Clague et al., 1989; Moore and Clague, 1992; Bergersen, 1995; Winterer et al., 1995; Thouret, 1999; Mitchell and Lofi, 2008; Staudigel and Clague, 2010]. The primary interest in these studies, for the purposes of this paper, is the observations of bathymetric highs found above erosional surfaces.

Some volcanic edifices, most notably those of the Hawaiian-Emperor chain, have been shown to experience a period of renewed volcanic activity after a long period of quiescence. This rejuvenated stage of volcanism is responsible for building late-stage volcanic cones, also known as posterosional cones, on top of islands, seamounts, and guyots from a number of island groups in the Pacific, including the Samoan Islands, Marquesan Islands, and Austral-Cook Islands [Sinton, 2009]. While these features have been observed on land and in bathymetric data for quite some time, the exact mechanism controlling when and where they develop is still uncertain. Some authors have suggested that posterosional volcanism originates from the periphery of the hotspot plume and is associated with plate flexure caused by seamounts regionally loading the lithosphere [Clague et al., 1989; Lonsdale et al., 1993]. Estimations for the duration of the volcanic hiatus prior to these rejuvenated eruptions have been made for many individual sites and tend to range from 1.5 to 10 million years [Staudigel and Clague, 2010]. Other investigators have found that instead of this posterosional volcanism stage following after a typical time interval, it should should occur at a characteristic distance from the shield volcano currently being built by the hotspot. For the Hawaiian-Emperor Chain, Clague et al. [1989] found that posterosional volcanic cones are built upon edifices which are about 190 km ± 30 km away from the location of the next large shield volcano being built. They believe this implies that a primary factor in rejuvenated stage eruptions is the rapid change from subsidence to uplift as the guyot overrides the flexural arch that is created [Clague et al., 1989; Lonsdale et al., 1993].

Other investigators have observed conspicuous, volcanic landforms rising above

erosionally subdued regional terrain on subaerial islands, guyots, and also continental volcanic settings [Cotton, 1952]. Most authors agree that differential erosion of volcanic products is the key process leading to these landforms, but the degree to which the erosionally-resistant rocks will be exposed is largely controlled by composition, erosion rates, and the specific geological setting [Thouret, 1999]. Differential erosion-formed topography may be subtle enough on some edifices that it is neglected, like for the Geisha Guyots [Vogt and Smoot, 1984], or severe enough to develop steep cliffs and plateaus rising several hundreds of meters like those found on islands of the South Pacific. Such subaerial landforms are interpreted to be volcanic plugs or necks which were so much more resistant to erosion than the neighboring volcaniclastic material, that they are all that remain after a long period of denudation [Cotton, 1952]. Morphologies falling in between these two end-members have also been observed. Erosional features have been identified on Valencia seamount which the authors believe were due to a period of subaerial exposure. The numerous small peaks occurring on its flanks near rift-arms are interpreted to be erosionally-excavated, resistant stocks which were fed by dikes radiating from the main volcanic core [Barone and Ryan, 1987; Mitchell and Lofi, 2008].

With the prevalence of carbonate reef growth on oceanic islands in the tropics, a number of studies have focused on the conditions and processes required to develop such bioherms. Carbonate reefs are known to develop where light, temperature, oxygen, and nutrient conditions are favorable for the survival of communities of benthic, calcite-secreting organisms. A main factor limiting the geographic range of these carbonate communities is temperature [Renema, 2002]. The metabolic rate of such organisms is

much higher in warmer water, and large symbiont-bearing foraminifera require minimum temperatures of about 16-18°C for the continued growth of their endosymbionts. Therefore, communities of benthic foraminifera which form carbonate reefs are expected to thrive only in the climatic zone limited by the 16°C isotherm for the coldest month [Langer and Hottinger, 2000].

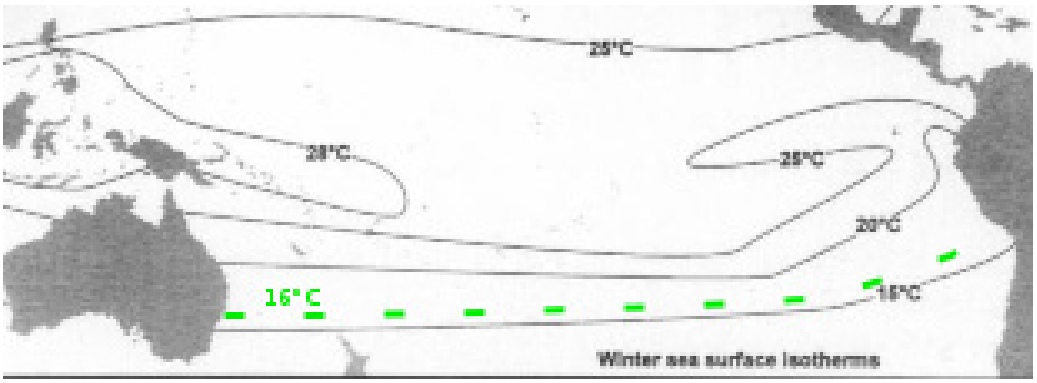

[Langer and Hottinger, 2000]

Figure 1: Sea-surface isotherms for the coldest month of the year;
inferred 16°C isotherm shown as dotted line

In Figure 1, present-day winter isotherms are shown for the southern Pacific Ocean. The dotted line representing the inferred location of a 16°C isotherm serves as an estimate for the southernmost possible extent for the survival of carbonate reef-building organisms in modern times. This line now crosses north of New Zealand near 30°S latitude. However, authors have described assemblages of carbonate-secreting organisms well outside of these geographical limits [Langer and Hottinger, 2000]. This is simply explained by the fact that air and water temperatures have fluctuated greatly over Earth's history.

The Eocene epoch was characterized by abnormally high temperatures. Paleo-

oceanographers have collected extensive $d^{18}O$ isotope data from the tests of benthic forams preserved in the deep-marine sediment column. The trends of these $d^{18}O$ values are then used to estimate changes in ocean temperatures in the past, identify periods of glaciation, and constrain the timing of other major climatic events [Bohaty and Zachos, 2003]. Based on the change from very low $d^{18}O$ values at the beginning to higher values at the end, the Eocene epoch is considered to have been a time of significant ocean cooling. Therefore, the isotherms shown in Figure 1 would need to be adjusted by about 6-9°C to represent conditions from the middle Eocene [Langer and Hottinger, 2000]. The presence of warmer waters at high-latitudes during the warm Eocene appears to have allowed communities of benthic organisms to expand their geographic extent. *Amphistegina*, a genus of large benthic foraminifera, for example, has been shown to have extended its range to 48°N - 36°S during Eocene times, compared to modern *Amphistegina* which are found from 34°N - 22°S [Langer and Hottinger, 2000]. If a comparable latitudinal shift in global range occurred for other large benthic organisms, then it is quite reasonable for many high-latitude guyots to have experienced carbonate-reef growth in the past.

The geomorphological expression of carbonate reefs varies greatly depending their extent and recent interactions with regional sea-level, and may lead to a range of classifications including atolls, proto-atolls, barrier reefs, and carbonate banks. The processes controlling their exact nature and classification are addressed by Winterer et al. [1995] and Winterer [1998].

Another process influencing the morphology of guyots which has been examined is tectonic deformation. Guyots experience significant amounts of mass

wasting around their flanks during the early stages of development, but the most severe tectonic deformations they encounter occur when moving through a subduction zone. Volcanic edifices approaching trenches have been observed to exhibit large fault scarps at which major vertical displacements have occurred. Two of the best-documented examples are the Daiichi-Kashima Seamount entering the Japan Trench [Konishi, 1989] and Osbourn Guyot which is moving into the Tonga-Kermadec Trench [Lonsdale, 1986].

1.3 REGIONAL SETTING

The Louisville Seamount Chain, previously referred to as the Louisville Ridge, is a trail of seamounts and guyots in the southwest Pacific Ocean that stretches over 4000 km long. Its oldest, northwestern-most end intersects with the Tonga-Kermadec Trench at about 25°S and trends southeast toward the presumed modern position of the Louisville hotspot near 50°S, 140°W (Figure 2).

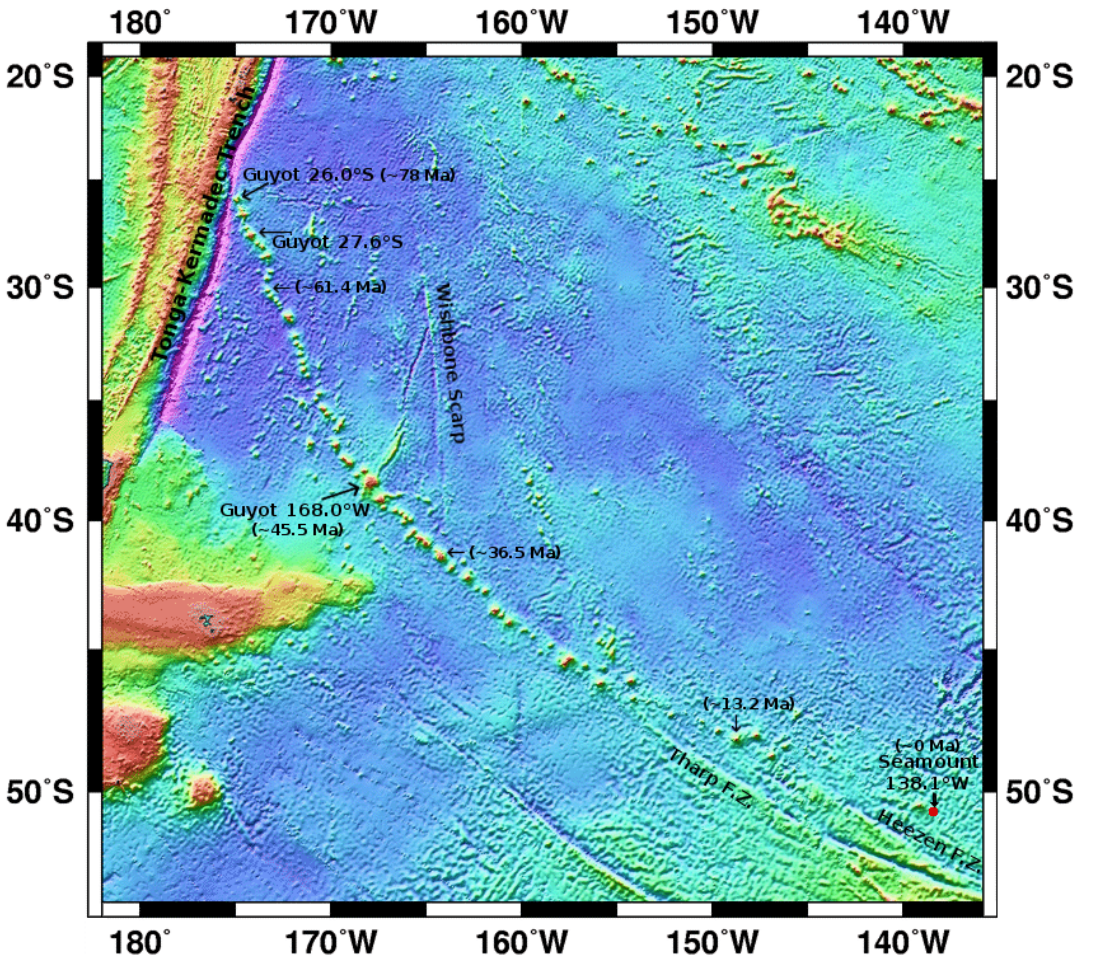

[1][Becker et al., 2009] ; [2][Koppers et al., 2004]

Figure 2: Regional map[1] of the Louisville Seamount Chain
with several guyots, large tectonic structures, and $^{40}Ar/^{39}Ar$ ages[2] labeled

Apparent trends in the nature of the seamounts and guyots have been identified. A reduction in the size and concentration of edifices from northwest to southeast seems quite clear from bathymetric data. It has been suggested that this could be reflective of a dying or waning Louisville hotspot [Lonsdale, 1988]. Most of the smaller guyots appear to have been evenly truncated by erosion at sea level, while the larger ones tend to be those with guyot summit plain peaks. This might result from a number of possibilities,

for example: there was too much material to be fully eroded in the typical amount of time spent at sea level; larger edifices are more likely to experience a rejuvenated stage; or larger edifices have better developed intrusive plumbing systems which are uncovered by erosion. A characteristic that may be unique to the Louisville chain versus other seamount trails that have been studied is that all of the lavas collected have been alkalic in nature; whereas, most intraplate volcanoes have been shown to experience stages of tholeitic lava production [Lonsdale, 1988; Thouret, 1999]. There does not appear to be any obvious trend in the azimuths or number of rift arms which develop, nor in the relative location of major slump scarps. The linear orientation and progressive ages of these volcanic edifices are likely the most informative trends seen for this system.

Portions of the chain are located in the vicinity of large-scale tectonic structures which may or may not have directly affected the development of the volcanic edifices. The Heezen and Tharp fracture zones obliquely intersect the southeastern-most reach of the seamount trail and could have contributed to the decline in along-chain volcanism. Upon crossing the fracture zones, the age and thickness of the lithosphere exposed to the underlying magma source increases significantly, thereby reducing the vulnerability of it [Lonsdale, 1988]. Another tectonic feature that intersects the chain is the Wishbone Scarp. While the significance of this structure is beyond the scope of this paper, the coincidence of its western branch with by far the largest guyot in the group, Guyot 168.0°W, likely suggests some association. The Tonga-Kermadec Trench, forming the northwestern boundary, has most definitely influenced the Louisville Seamount Chain. Not only are the guyots deformed as they move into the trench, there is direct evidence

that the trench has already consumed one or more edifices which were older than Guyot 26.0°S (Osbourn Guyot), thereby removing the earliest evidence of the hotspot's influence [Lonsdale, 1986]. An index map showing the along-chain locations of each individual figure and plate is included as Plate 1 in order to provide a better understanding of the spatial relationships discussed in this study.

2

Data & Methods

Geologic interpretations presented in this study are based primarily on geophysical data collected aboard the *Roger Revelle* during the AMAT02RR expedition in early 2006. Previously available regional bathymetry data was gathered by the 1972 and 1984 expeditions aboard the *Thomas Washington,* with lower-resolution Seasat altimetry filling in the missing data. The types of data processed and interpreted for the purposes of this study include: multibeam bathymetry with associated amplitude data, multichannel seismic reflection data, 3.5 kHz Knudsen CHIRP data, and collected dredge samples. The specific processing schemes applied to each type of data are addressed below.

2.1 MULTIBEAM BATHYMETRY DATA

Bathymetric and reflectivity mapping of the Louisville seamounts, guyots, and regional seafloor was accomplished with an EM120 multibeam echo sounder. This system utilizes frequencies ranging from 11.25 kHz to 12.75 kHz, covering up to 150 degrees. Ideally, the EM120 should be capable of measurement accuracy on the order of 0.2% of depth RMS, which translates to a 10 m resolution at 5000 m depth [British Antarctic Survey, 2008]. Interpretations were not made at this level of resolution, however, since there is a significant amount of noise in the outer beams.

The bathymetric data presented in this paper was processed and displayed using a combination of MB-System and GMT programs. All of the bathymetric maps shown were produced using 50-200 m grid spacing, depending on the scale and amount of noise in the data. For instances in which higher resolution was necessary to make small-scale observations, an MB-System program called MBedit was used. This allows

analysis on a ping-by-ping basis and is the highest possible resolution that can be used for interpretation. The EM120 system also allows isolation of the amplitude of the signal to effectively produce reflectivity maps. These maps yield valuable information about the hardness of material encountered on the seafloor, thus providing clues to the potential lithologies that are present. Much care must be taken when interpreting reflectivity data since the signal is also partially a function of the angle of incidence.

While qualitative, the criterion used in this study for the designation of guyot summit plain peaks is simply any feature which significantly disrupts the generally flat, smooth summit platform as resolved by bathymetric data. The specific nature of each of these features is interpreted based on the morphological characteristics observed, along with their compositions. For example, steep, narrow cones are considered to be indicative of submarine volcanism, while broad domes or bulges are likely to be the erosional remnants of more resistant rock. Tectonically produced features can be recognized by systems of linear fault-scarps with fairly uniform azimuths. Biogenically built structures are less straight-forward morphologically, but may appear as flat platforms, neighboring mounds, or perimeter ridges.

2.2 MULTICHANNEL SEISMIC REFLECTION (MCS) DATA

During the 2006 expedition, the *Roger Revelle* utilized a multichannel seismic reflection data acquisition system with generator-injector (G.I.) air guns as the seismic source. The towed array of two G.I. air guns with 45/105 in^3 capacities produces seismic pulses which are reflected off of the seafloor and subsurface interfaces. These reflected signals are then collected by a 48-channel streamer which gets towed further behind the

seismic source. Numerous post-processing steps are required to correct for physical phenomena and produce the most representative profile possible. For this study, processing techniques were performed using a combination of Seismic Unix and SIOSeis. These techniques included CDP sorting, bandpass filtering, detailed semblance velocity analysis, normal move-out correction, data stacking and migration, water column muting, and time varied gains. Finished seismic profiles are shown using a red and black color scheme with 4x vertical exaggeration.

For the specific purposes of this study, the MCS data was most useful for the interpretation of biogenically produced peaks. These features, including their subsurface structures, were clearly imaged in the seismic reflection data, while volcanically-dominated settings tended to yield very little structural information. High-resolution seismic reflection data are considered invaluable for studies located in regions with a lot of sediment, but the heterogeneous nature of volcanics limits its usefulness. Once the seismic energy reaches the volcanic interval, it is scattered in many directions preventing the return of any informative reflections. Overlying beds of sediment are clearly imaged as continuous, alternating reflections representing positive and negative impedance change across layer interfaces; however, once the volcanic basement is reached, only chaotic reflections can be seen. Acoustic basement is considered to be the lowermost, laterally-coherent reflection and is most often attributed to a hard volcanic unit.

In the case of post-planation volcanic peaks, seismic reflection data are of especially little use. The combination of heterogeneity, high-amplitude reflection, roughness, and steeply-sloping structure of these types of peaks makes it impossible to

decipher anything from the returned seismic signal other than chaotic hyperbolas [Anstey, 1977]. One piece of information that may be gleaned from this data, however, is the regional thickness of material above the erosional surface, which may be informative of volcaniclastic deposition and prevailing currents. Another hindrance to seismic interpretation of many of these features occurs due to side-echoes produced by the shiptrack not crossing directly over the summit a peak or the presence of nearby peaks.

Seismic reflection studies performed in the marine environment are often hindered by the difficultly associated with differentiating between volcanic and carbonate units. Both lithologies can return relatively laterally-coherent reflections and are characterized by high compressional velocities. Further complicating the interpretation, varied levels of alteration and diagenesis are often present which act as primary controls on the rocks' physical properties [Kenter and Ivanov, 1995]. Yet there are some observations that have been made in the literature concerning how carbonate reefs and mounds should appear in seismic reflection data [Sheriff, 1975; Anstey, 1977; Fontaine et al., 1987]. Carbonate platforms may exhibit low-amplitude, horizontal reflections while more isolated carbonate pinnacles are often represented by a zone of very subtle reflections at which laterally continuous reflections terminate on either side. Homogeneous limestone deposits generally appear as high-amplitude, continuous reflections at the top and base with a reflection-free zone in between. The appearance of nearby reflections with high rugosity is another good indication that there are carbonate reefs present since they are often thought to represent reef-debris and talus [Fontaine et al., 1987]. Carbonate deposits also transmit seismic energy through them more

efficiently than basalt flows, so the reflections representing volcanic basement are often resolved below the carbonate sequence.

2.3 CHIRP – 3.5 KHZ KNUDSEN DATA

Along with the lower frequency multichannel seismic system, the ship was equipped with high frequency (3500 Hz) CHIRP sonar which also records subsurface information. Thin beds and small-scale structures are not imaged as clearly as with the multichannel seismic system, but this data is quite useful for distinguishing sediment cover from basement and also filling in gaps in seismic data since this system is run nearly continuously throughout the cruise. The digital form of this data was also processed using SIOSeis. The quality of the CHIRP data from this expedition is quite poor since the pings were intentionally limited so as not to interfere with the EM120 multibeam echo sounder. The hard, reflective nature of the material present on the guyot summit plains further inhibits the usefulness of this type of data.

2.4 DREDGE SAMPLES

A select number of dredge hauls have been performed on the guyots of the Louisville Seamount Chain during past cruises. The best sample coverage comes from the AMAT02RR expedition in 2006, but in order to get comprehensive coverage of all of the guyots in this study, supplementary data from the German dredging cruise SO167 that took place in 2003 is used. The dredging strategy for SO167 and much of AMAT02RR, in which large scarps on the guyot flanks were the primary targets, is not ideal for this particular study of peaks built above guyot summit plains. Rock sample

identification was performed by the shipboard scientists of each expedition, and no additional examination was made for this paper.

Absolutely imperative to any geophysical study is the groundtruthing of data by means of collecting geological samples, most commonly performed in the marine environment by deep-sea drilling or dredge hauls. This study suffers from a complete lack of drilling data, but a number of dredge samples have been collected over most of the length of the Louisville Chain. Samples from specific sites are incorporated into the interpretations of this study as much as the data coverage allows. The types of lithologies expected to accompany secondary cones are typically extrusive lavas flows and volcaniclastics with a range of alteration states depending on the degree and duration of exposure to sea water. Samples collected from erosional remnants would be expected to be primarily highly-resistant rock types with larger crystal structures and perhaps more severe alteration. Or given the highly-indurated nature of these plutonic rocks, poor recovery of dredge hauls in general should be expected. All of these samples are likely to be encrusted with variable amounts of ferromanganese-oxides, depending on the specific regional conditions.

3

Discussion

3.1 BUBBLE PULSE MULTIPLES IN MCS DATA

The multichannel seismic reflection profiles for nearly every surveyed Louisville guyot display a signal which appears very similar to a bottom-simulating reflector. This signal is observed crossing primary reflections on some profiles (Figure 3), which indicates that it is likely an artifact in the data or possibly a diagenetic horizon. The fact that an array of G.I. air guns was used should diminish the likelihood of this signal being a bubble pulse artifact. However, if the timing between the generator and injector is slightly off, the collapse of the primary bubble pulse may not be dampened adequately, which could lead to a bubble pulse multiple [Landro, 1992]. Recent reprocessing of select MCS profiles, which incorporated a wavelet reshaping step, successfully removed this data artifact, thereby verifying that it was in fact a bubble pulse multiple. This artifact would not be considered a true bottom-simulating reflector, however, since it is not always associated with the actual water bottom, but rather is found deeper in the subsurface in some areas (left side of Figure 3).

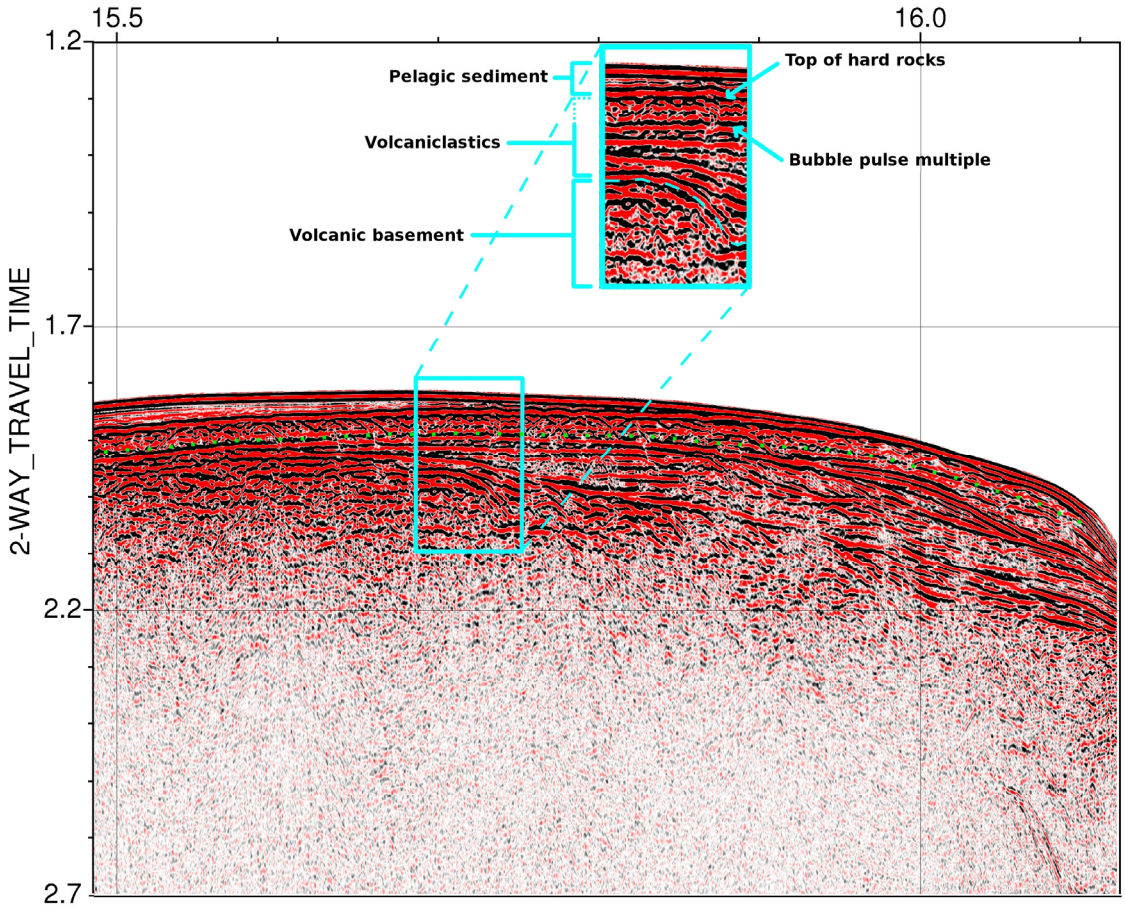

Figure 3: MCS Profile 27.6-6 displaying the bubble pulse multiple in the subsurface

There is also a strong correlation of high reflectivity, observed in bathymetric data, with regions exhibiting the bubble pulse signal. Figure 4a shows reflectivity data which demonstrates the highly reflective, hard nature of most of the material shallower than about 550 mbsl on this guyot. Those same regions of high reflectivity can be seen in the seismic profile of Figure 4b as having a strong bubble pulse present in the near subsurface. This indicates that bubble pulse multiples only appear where the seismic energy has encountered very hard material. Thus, the presence and relative location of the bubble pulse multiple may actually provide additional information which aids

geological interpretation. Areas clearly displaying a strong bubble pulse at the guyot surface may be interpreted as having hard rock present very near the water-seafloor interface. Conversely, the lack of a bubble pulse in the shallow subsurface indicates that region of the guyot surface is composed of soft sediment, and any reflection lower in the subsurface that is associated with a bubble pulse is likely the uppermost hard rock layer. The interpretation that regions lacking a bubble pulse signal near the guyot surface are composed of thick sediments is supported by the observation of thin, low-amplitude, highly-continuous reflections, as can be seen on the left side of Figure 3.

The highly-indurated nature of the material causing bubble pulse multiples is illustrated by the fact that erosional channels, which have developed on the northwest section of Guyot 168.0°W in the pelagic sediments, are unable to penetrate into it, thereby forming the channel bottoms. Also demonstrative of the hard nature of these materials, they act as acoustic basement in the 3.5 kHz Knudsen data; although this is at least partially due to the fact that Knudsen pings were limited during the AMAT02RR cruise.

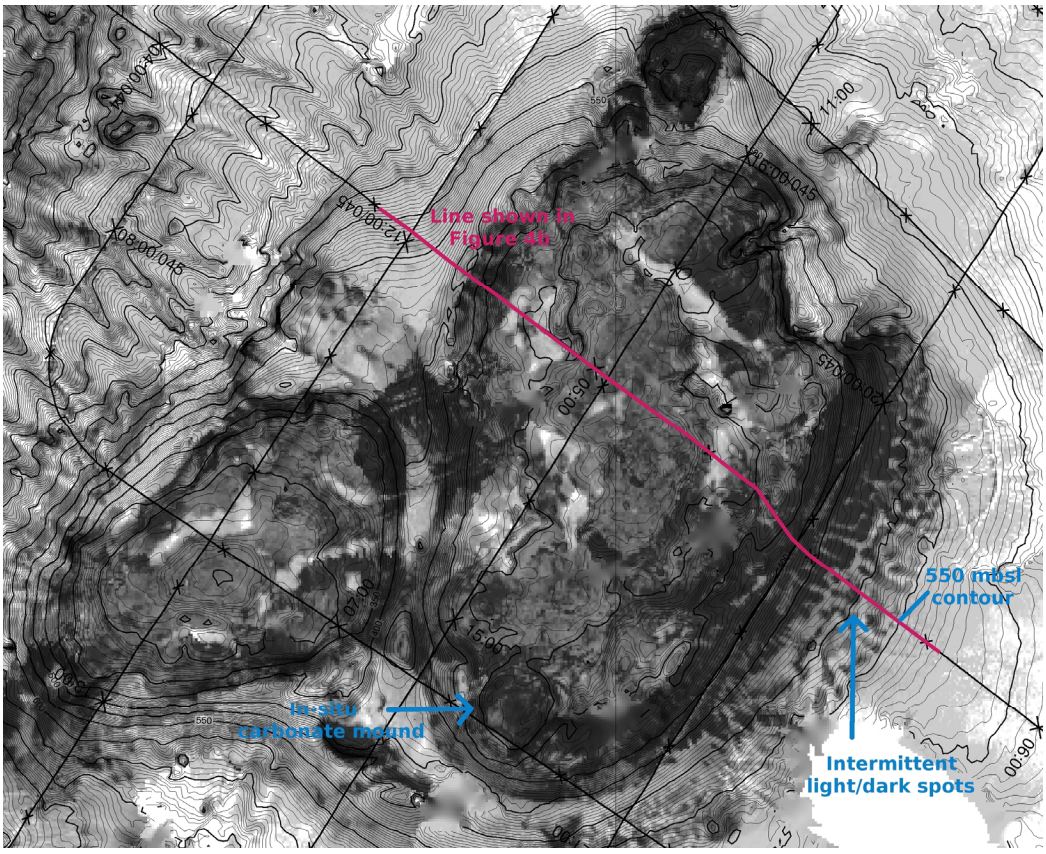

(a)

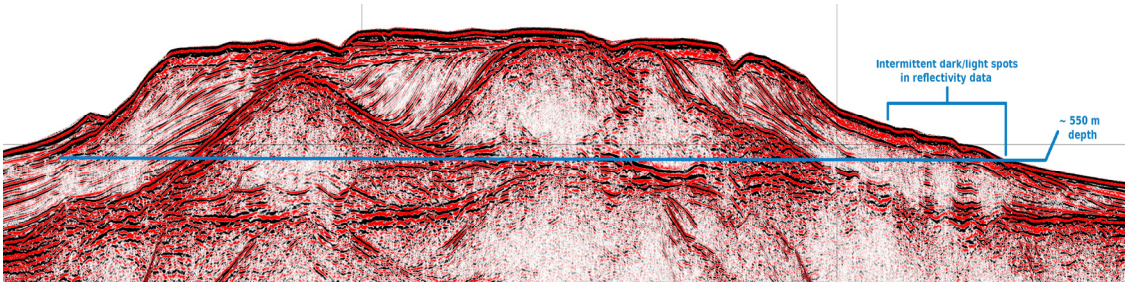

(b)

Figure 4: (a) Small-scale map of Guyot 168.0°W reflectivity data (same aerial extent as Figure 14); (b) Section of Profile 168.0-1 demonstrating the correlation of high reflectivity (dark areas) with the near-surface bubble pulse multiple

3.2 FLUID FLOW & LITHIFICATION OF GUYOT SURFACES

There is little doubt that while submarine intraplate volcanoes are actively erupting, there is associated fluid flow occurring in the near subsurface driven by a large thermal gradient. However, the idea that seamounts continue to experience significant fluid flow tens of millions of years after activity has ceased remains an active topic of research [Rougerie and Fagerstrom, 1994; Harris et al., 2004; Judd and Hovland, 2007; Staudigel and Clague, 2010]. Many investigators have been attracted to seamounts and guyots as potential long-lived fluid flow pathways because of their relatively sediment-cover free nature and the high porosities and permeabilities associated with the extrusive material. Most agree that the vigorous hydrothermal venting that occurs while these edifices are volcanically active cannot be maintained for long after the heat source dies off. Instead, water may be drawn into the outer permeable portion of the edifice either at mid-depths by endo-upwelling [Rougerie and Fagerstrom, 1994] or near the base due to the significant bathymetric relief which generates thermal buoyancy forces in excess of the seafloor [Harris et al., 2004]. The endo-upwelling model is still driven by a hot volcanic pedestal, while the thermal buoyancy force model only requires very small temperature gradients. Judd and Hovland [2007] agree that a hot volcanic pedestal is not required for continued fluid flow through seamounts. They interpret that seawater could be drawn in from the surrounding seafloor, circulated like any other hydrothermal solution, and eventually expelled at the summit.

Assuming that there is in fact a mechanism capable of driving long-term fluid flow, an explanation for the apparently sporadic appearance of high-reflectivity areas present on the guyot summit plain surface can be hypothesized. It is possible that the

hard material associated with the bubble pulse multiples and “white-out” zones directly beneath them was formed by the presence of previously migrating fluids. As these mineral-rich solutions migrate towards the guyot summit plain through fractures and permeable sediment beds, they experience changes in water temperature and pH which may cause some minerals to come out of solution to promote regional cementation of sediments [Judd and Hovland, 2007]. The underlying reflections are lower amplitude because the hard material at the surface, interpreted here as a result of lithification by mineral-rich fluid flow, has attenuated much of the high frequency signal.

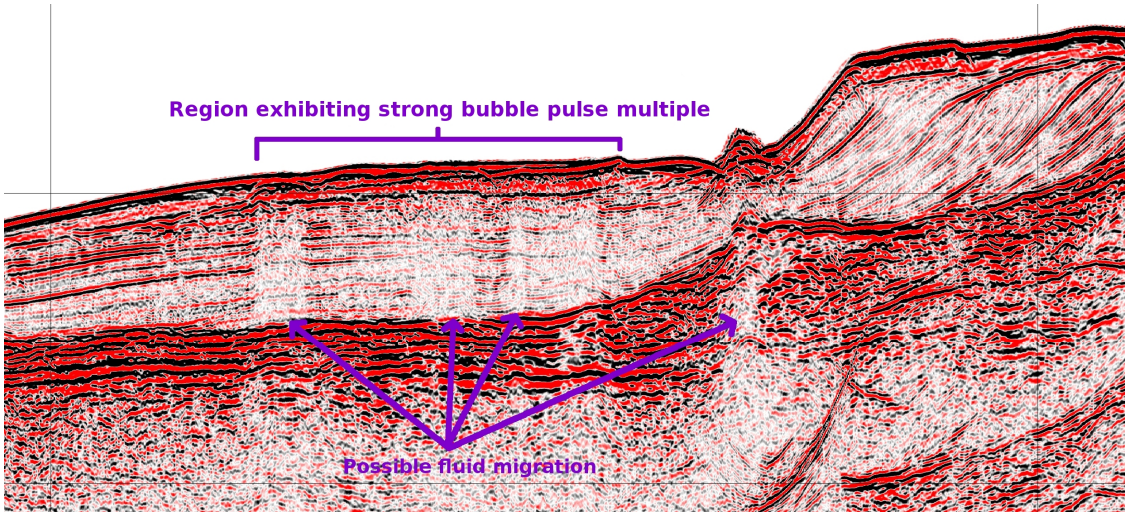

Figure 5: Section of Profile 168.0-8 showing potential evidence of material lithification encouraged by previous fluid flow

3.3 MULTIPLE ORIGINS OF LOUISVILLE GUYOT PEAKS

3.3.1 Peaks of Constructional Volcanic Origin

Based on the characteristic structures and compositions that late-stage volcanic eruptions are known to produce in previously studied subaerial and submarine settings, it is possible to infer what geophysical expression they are likely to exhibit for this study. If a point source is assumed for erupting lavas, deep submarine volcanoes will generally form steeply-sided conical structures composed largely of pillow basalts. Hydrostatic pressure allows these features to retain steeper flank slopes than their subaerial counterparts, however the specific dimensions of such cones can vary widely depending on eruption depth, duration, and composition [Bonatti and Harrison, 1988]. Shallow eruptions (<700 m depth), which are expected to be the most common type occurring on rejuvenated-stage guyots, are dominated by explosive and mechanical fragmentation of lavas to produce volcaniclastic material. These hydromagmatic eruptions often produce highly-vesicular scorias and pumice that lack the fine grain-size fraction, which remains suspended and is transported away by turbulent waters [Staudigel and Clague, 2010]. A morphological study of late-stage alkalic cinder cones on the Mauna Kea Volcano in Hawaii shows a relative uniformity of the cones' slopes. Of the over 300 cinder cones studied, nearly all of them had steep flank slopes consistently ranging from 25° to 27° [Porter, 1972]. These subaerially erupted cones were built in the absence of a hydrostatic confining force, which should lead to lower slopes, but the lack of water currents to transport the erupted material away from the source has the opposite effect. Similarly, posterosional volcanic cones built on the guyot summit plains of the Louisville Seamount Chain should be expected to appear as

relatively steeply-sided, conical features composed of low-density material which may have cratered summits. Considering that these types of volcanic cones are never exposed to subaerial erosion, they are expected to retain any angular features as well.

A good example of post-planation volcanic cones on the Louisville Seamount Chain is shown on the multibeam bathymetry map of Guyot 165.4°W in Figure 6. Steep, narrow cones in a range of sizes can be seen covering much of the edifice. The dimensions and slopes of these cones were measured using Fledermaus, two of which are shown in Figure 6 with diameter measurements displayed as examples. The smaller cone demonstrates a vertical change of 100 m over its 0.6 km base diameter which gives its flanks average slopes of 18° and has a maximum slope of 31°. The other cone has just over 200 m of vertical change over a horizontal distance of 1.4 km, thereby yielding average flank slopes of roughly 16° and a maximum slope of 23°. A summary of the ranges in average and maximum slopes measured for the peaks on each guyot are shown in the table attached as Plate 2. Even though there is significant scatter in the slopes observed on this guyot, they each fall into the range (average slopes >15°) that would be expected for a constructional, submarine volcanic cone. Additionally, large-scale drainage features appear to have developed around the main erosional platform, which is controlled by its intrusive core, but not around the individual peaks themselves. This also provides strong evidence in favor of a constructional volcanic origin for the peaks.

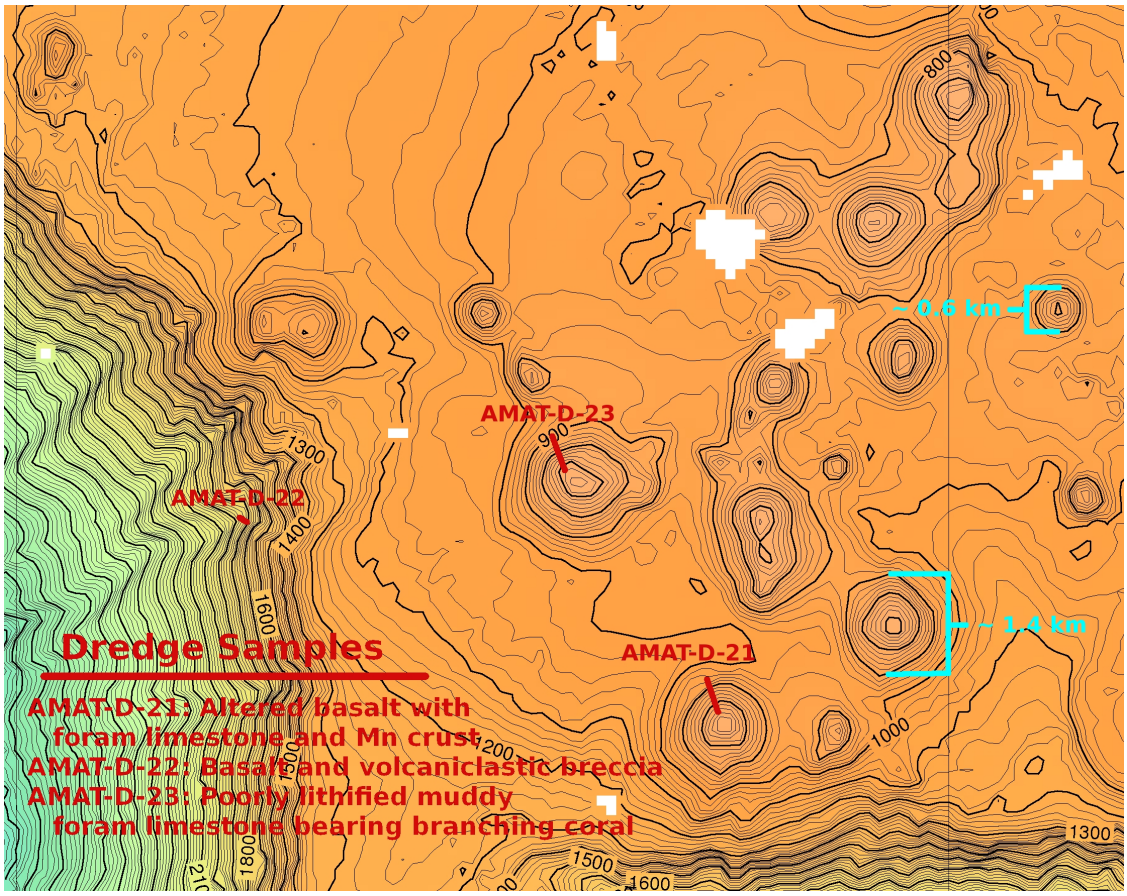

Figure 6: Bathymetric map of constructional volcanic cones on Guyot 165.4°W

The bathymetric map of Guyot 165.4°W shown in Figure 6 also displays three dredging stations with the sample lithologies listed. There were two dredge hauls collected on the summit plain peaks of this guyot, but the material collected was not conclusively indicative of a constructional or erosional origin. The foram limestones simply represent the accumulations of planktonic foraminifera tests which have been lithified over time.

Other examples of post-planation volcanism in the Louisville Chain can be seen on Guyots 26.5°S and 26.6°S. For the most part, these edifices display very similar

conical features to those found on Guyot 165.4°W, with average slopes and maximum slopes agreeing quite well. However, evidence suggests a few of the peaks on Guyot 26.6°S (Figure 7) may in fact be transitional in nature. They might represent post-planation cones which developed early on enough to build up to sea level such that the upper portions of these secondary cones were partially shaped by wave erosion.

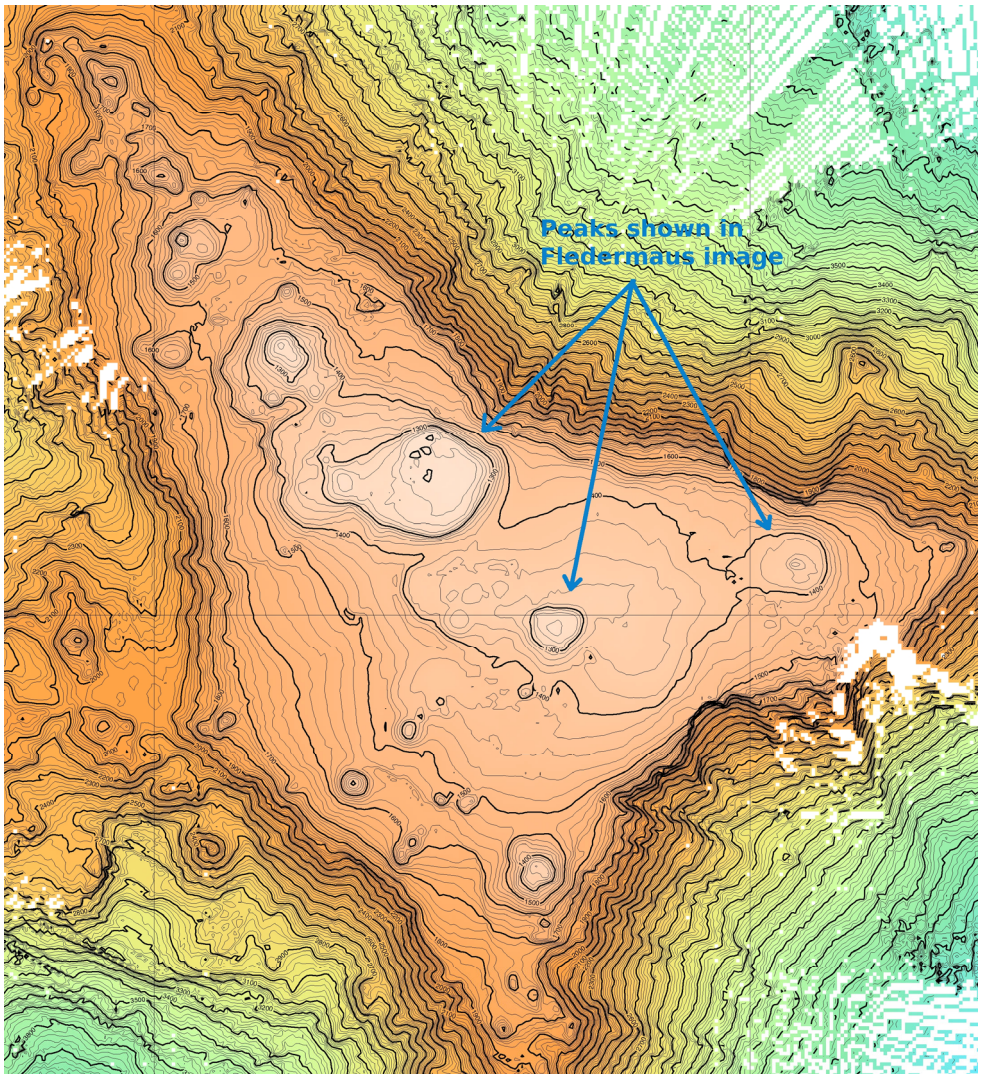

Figure 7: Bathymetric map of Guyot 26.6°S showing constructional peaks and potential transitional peaks

Northwest of the main edifice core, a broad peak is observed with an irregular, rounded summit (Figure 7). The morphological expression of this specific peak, which also happens to be the guyot's shallowest point, indicates that it developed in a different manner than most of the peaks adjacent to it. While not immediately clear from the gridded bathymetry data, a closer evaluation of this and two other peaks which diverge from the typical constructional shape using MBedit seems to show that small shelves or platforms appear to have been cut into their upper summits (Figure 8a). This observation is more clearly shown using Fledermaus in Figure 8b. While these are the only peaks identified here to demonstrate this pattern, similar features may exist on other Louisville guyots as well.

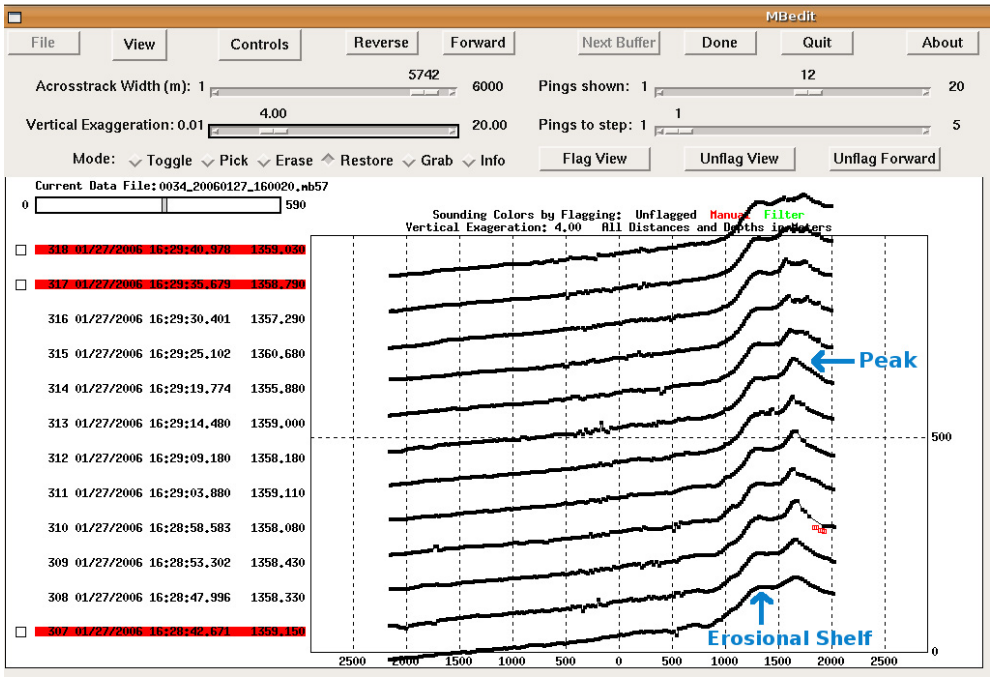

(a)

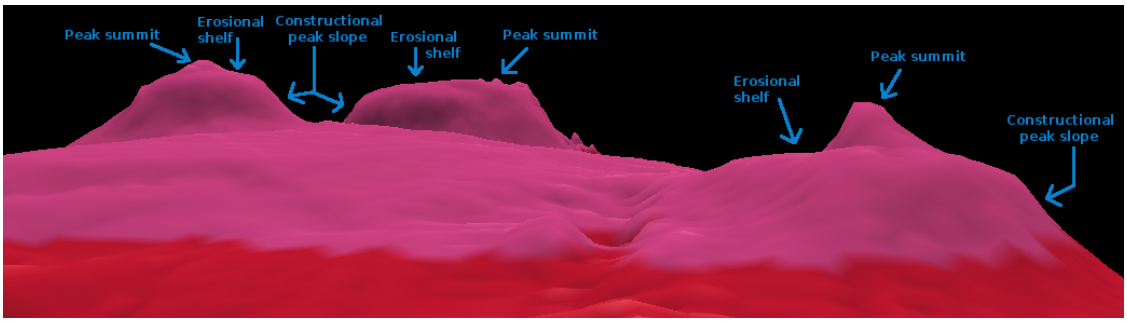

(b)

Figure 8: (a) MBedit screenshot showing suspected erosional shelf on summit peak from 26.6°S; (b) 3D Fledermaus view of high-resolution bathymetric data displaying transitional peaks

3.3.2 Peaks of Erosional Origin

Another mechanism that has been postulated to explain peaks rising above guyot summit plains is differential erosion [Vogt and Smoot, 1984; Barone and Ryan, 1987; Lonsdale, 1988; Mitchell and Lofi, 2008]. As oceanic island volcanoes are built, they experience a complex interplay of intrusive and extrusive volcanism which causes rapid regional changes in lithology throughout the edifice. The basic model for these edifices' structures is that, while active, they continually grow from the inside-out by intrusively emplacing dikes and sills, while also growing upward and outward by extrusive volcanic deposition [Contreras-Reyes et al., 2010]. At the height where guyot summit plains are erosionally formed, only the uppermost intrusive plumbing system is likely to be exhumed. These intrusive conduits cool slowly producing highly-resistant types of plutonic igneous rock, while the outer parts of the volcanic edifice, which are composed of extrusive flows and volcaniclastic deposits, will be much more susceptible to erosion.

As seamounts subside, both subaerial and littoral erosion work quickly to remove the more porous volcanic tuffs and ash layers, which in turn often undercuts extrusive flows, further promoting the removal of extrusive products. Toward the central part of the edifice, a volcanic plug representing the primary magma conduit would be much less affected by erosion because it has a more resistant composition, is less fractured, and benefits from the thick barrier of extrusive volcanics which must be removed before being exposed to erosion. If an intrusive plug is present at the level that gets planed off, a broad bulge near the guyot center will be exposed [Scarth, 1994]. Further evidence for an erosional origin of peaks, which may be found in bathymetric data, is the development of deep erosional channels around these structures. While

erosion is shaping the inner portion of the guyot, drainage channels develop in the weaker material to form pathways leading downslope from the erosionally-resistant plugs. Such well-established drainage features would not be expected around constructional peaks since they would have developed after the subaerial erosional stage was complete, and submarine scour requires initiation by slope failure of pelagic or bedrock materials, which cannot be reliably established here [Mitchell and Lofi, 2008].

Many of the bathymetric expressions expected for erosionally-developed peaks addressed above are demonstrated in Figure 9 for Guyot 27.6°S. This small-scale view of the guyot summit displays rounded, subdued peaks with well-developed drainage channels having formed around them. The dimensions and slopes of the peaks on this guyot were measured, two of which are for shown here, for comparison to those thought to be of constructional origin. The larger peak on the left exhibits an 80 m vertical change over its 2.1 km wide base. This gives its flanks average slopes of only about 4.5°. The peak on the right side of Figure 9 has a vertical increase of 65 m over a 1.7 km wide base, thereby yielding average slopes of 4°. These slopes are much lower than those seen for peaks interpreted to be of constructional origin. Also, these 4-4.5° slopes are average values and do not represent the nature of the actual slopes at those peaks. The instantaneous slope is really much steeper around the periphery and quite subtle toward the center. This is exactly what should be expected for an exhumed volcanic stock based on observations from subaerial volcanic erosional remnants. Well-indurated volcanic breccias, interpreted to be the erosional residuals of magma conduits, often form large-scale isolated landforms on volcanic islands, generally exhibiting rather steep cliffs around the perimeter and relatively flat tops [Scarth, 1994]. The linear

grouping of peaks seen toward the middle of the figure may be the result of a vertical dike having been eroded, but no evidence for a subaerial counterpart to this has been observed. A bathymetric map of the entire Guyot 27.6°S complete with dredging site locations is included as Plate 3.

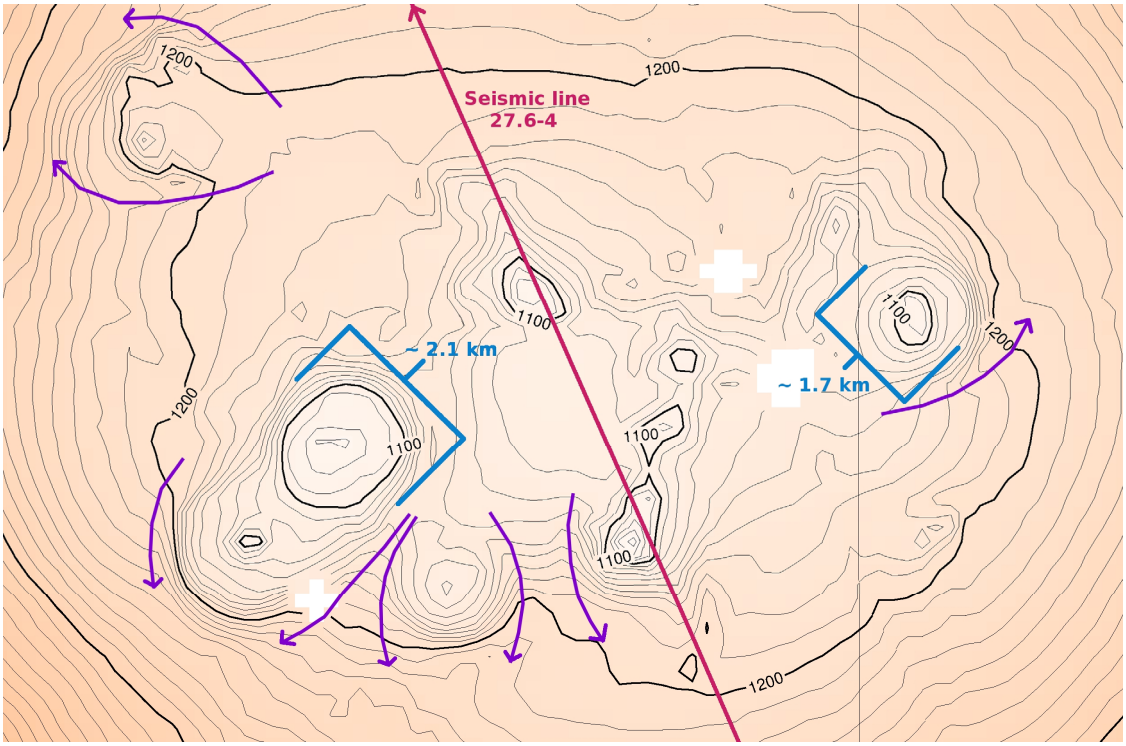

Figure 9: Small-scale bathymetric map of erosional peaks on Guyot 27.6°S

For an erosional interpretation to be correct, the surface of the guyot summit plain must represent roughly the same condition it was in when it subsided below wave base, except for the thin pelagic sediment cover. MCS data allow observation of a horizontal slice through the in-situ volcanic structure. While acoustic basement is reached almost immediately toward the center of the guyot, the outer portions display

thick sections of laterally-coherent reflections (Figure 10). This is interpreted to be the transition from intrusive or massive lava flow rock types to volcaniclastic material, and may be further delineated by a subtle change in slope at the summit plain surface. This occurs because wave erosion is able to cut into the volcaniclastic outer section much more rapidly than the resistant hard-rock core. The full seismic line 27.6-4 included as Plate 4 effectively demonstrates both of these observations.

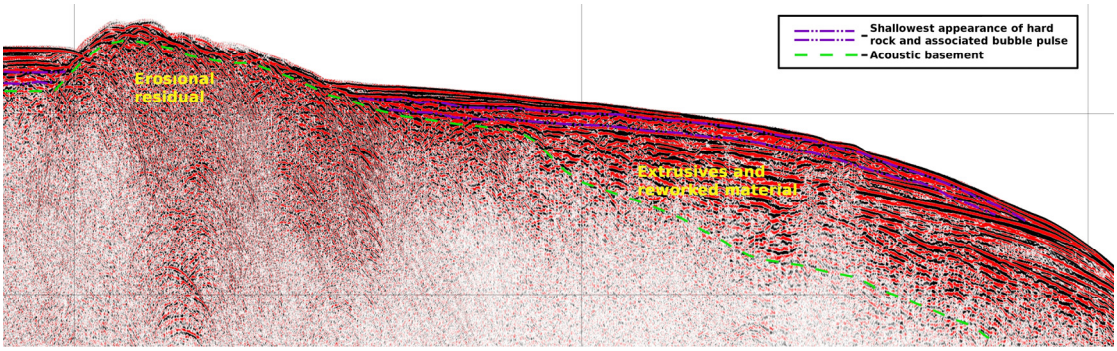

Figure 10: MCS data from Guyot 27.6°S (small-scale view of Profile 27.6-4)

Thick, prograding sections can be seen in the subsurface of the outer summit plain that pinch-out against the central intrusive core upon which the erosionally-shaped peaks are found. The subtle transition in slope due to change in lithology is shown best on the left side of the 27.6-4 profile (Plate 4) at about 9.5 hours (x-axis), where the acoustic basement, representing eroded intrusive core, can be seen cropping out beneath contour-smoothing pelagic sediment. The profile shape of the central peaks seen on seismic line 27.6-4 appears to show more subdued outer peak slopes compared to the steep, central-facing slopes, which seems to illustrate the differential effect of littoral

erosion on exposed rock faces compared to the protected ones. However, this is actually just an illusion created by the chosen shiptrack. A more careful analysis of the peak slopes on Guyot 27.6°S in bathymetry data (Figure 9) shows that there is no significant difference in slope from one side to the other.

Reflections representing regionally varying thicknesses of reworked pelagic sediments are seen directly overlying the hard rock material which causes the bubble pulse multiple. Pelagic sediment thickness trends (Figure 3) seem to suggest a system of paleocurrents which either caused preferential deposition on the southeastern portion of the guyot or remobilization of sediments from the more northwesterly section to deposit them further southeast. The apparent lack of a clear bubble pulse multiple in the area of the erosional residual (Figure 10) is due to obscuring diffraction hyperbolas, and reflects the hard, highly-scattering nature of the material. Figure 10 also displays the transition from sedimentary and volcaniclastic layers to the erosional residual rock outcrop near the center of the summit plain surface.

Dredge samples taken from Guyot 27.6°S did not contribute significantly to this interpretation. The only dredge performed on one of the interpreted erosional peaks, AMAT-D-2, yielded a poorly-indurated fossiliferous limestone which is thought to have developed since submergence following deposition of planktonic sediments. Available dredge samples from the flanks of the guyot are mainly breccias composed of a range of lavas from olivine-plagioclase phyric basalts to aphyric basalt. While dredging results do not definitively demonstrate an erosional origin of the peaks, the fact that there was such poor recovery of volcanic rocks from the dredged peak may reflect the hard, resistant nature of such erosional remnants.

3.3.3 Louisville Guyots with Constructional and Erosional Peaks

As might be expected, these two origins of peaks are not mutually exclusive. It appears to be quite common for peaks on one section of the guyot to be erosional in origin while those of another section are constructional. Peaks which have developed due to differential erosion are anticipated to be situated over or very near the main core of the edifice, however not all peaks over the central portion are necessarily erosional in origin. Peaks located near guyot edges are more likely to be representative of post-planation volcanic cones since the primary magma conduit system is restricted to the volcanic core and rift arms.

Guyot 169.0°W is a complex edifice formed by the bridging of two independent guyot cores by a long NW-SE trending ridge. The guyot summit plain, for both edifice centers and the connecting ridge, is largely defined by an erosional surface present right at the guyot-water interface with a generally thin overlying pelagic sediment cover. This basic structure is clearly interrupted in two regions: the southwest section of the northern guyot core and near the southwest rift arm of the southern guyot center. These two distinct structures which interrupt the generally smooth contours of the summit plateau are shown in Figure 11. A map of the entire guyot which also shows the position of seismic line 169.0-3 is included as Plate 5.

The subtle bulge located on the northern guyot center (Figure 11a) is made apparent by the development of drainage channels on either side of it. These channels along with the broad, smooth plan shape suggest an erosional origin for this feature. The 1100 m depth contour appears to closely follow the transition from more erodible extrusives to the residual intrusive material. Measurements of this structure for slope

estimation show about 50 m of vertical change over the 1.65 km wide base. These values yield a flank slope average of 3.5°, which is comparable to the 4-4.5° average slopes of the peaks on Guyot 27.6°W of erosional origin. The more obvious peak seen on the southern guyot center (Figure 11b) interrupts the primary summit plan shape even more significantly in that a cone with about 200 m of relief above the summit break in slope is present. This change in depth occurs over a roughly 1.9 km base, giving a slope average of 12° and maximum slope angle of 22°. The relative location, angular features, and much greater average and maximum slopes of this structure support a constructional volcanic origin for this peak.

(a)

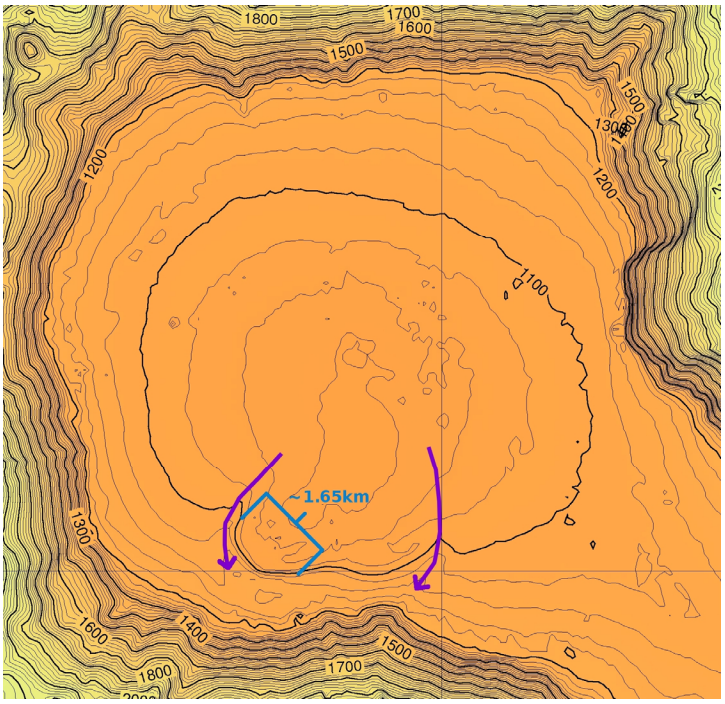

(b)

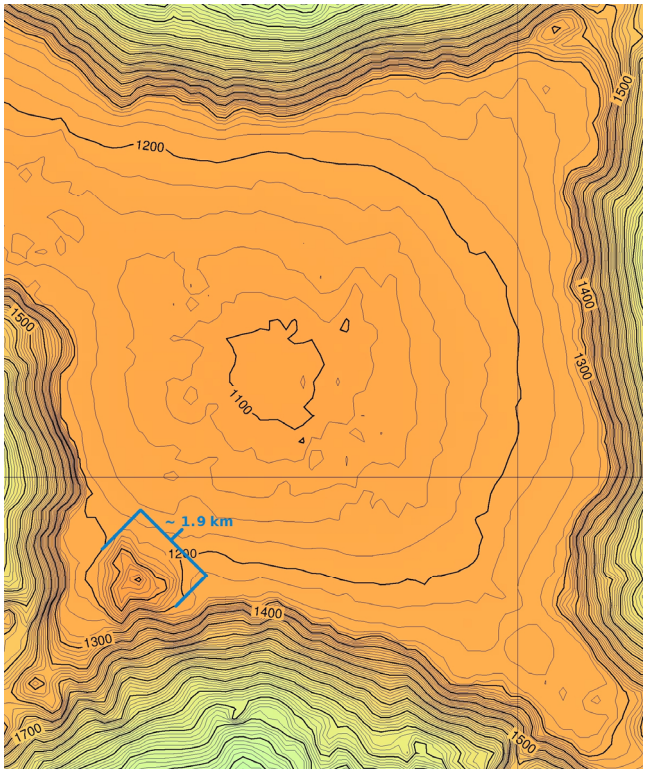

Figure 11: (a) Bathymetric map of erosional remnant on the northern portion of Guyot 169.0°W; (b) Map of constructional volcanic cone on the southern portion of Guyot 169.0°W

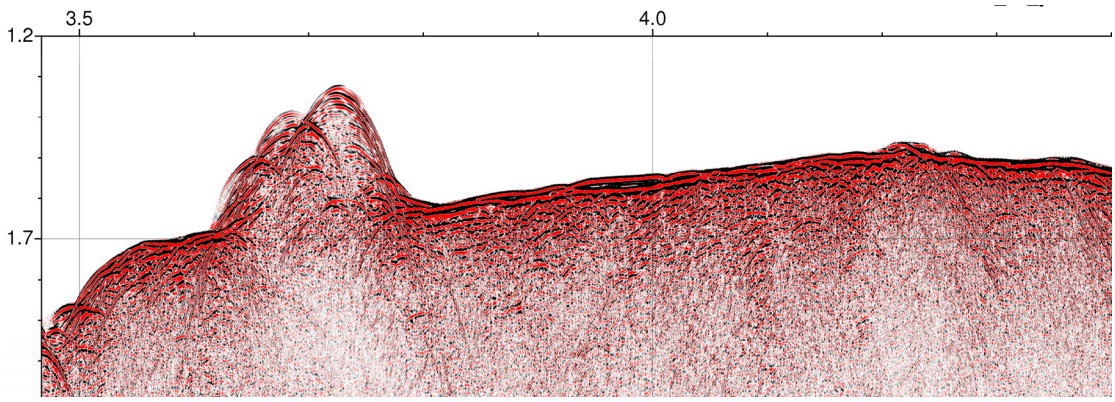

Figure 12: Constructional peak on Guyot 169.0°W as seen in MCS data

The seismic reflection example in Figure 12 shows the main erosional platform draped by pelagic sediment, along with a constructional volcanic peak which is represented by chaotic hyperbolas due to its steep sides and angular features. The seismic energy arriving at the cone is scattered such that the internal structure of the secondary volcano and the original surface it is presumed to have been extruded through cannot be imaged.

The SO167 cruise collected a few dredge hauls from this guyot, but they add little to the interpretation of guyot summit peaks since no samples were collected on or near the apparent constructional volcanic cone. Dredges performed around the guyot perimeter, below the break in slope, yielded a variety of lavas and breccias. Lavas and clasts present were aphyric basalts and olivine-pyroxene basalts with a range of vesicularities and weathering states.

3.3.4 Peaks of Tectonic Origin

Guyots and seamounts are generally believed to ride passively along with the lithospheric plate they are erupted upon, with the majority of their faulting and mass wasting having completed during or shortly after the final stage of volcanism ceased [Moore and Clague, 1992; Thouret, 1999; Staudigel and Clague, 2010]. However, with seafloor spreading acting as a continuously recycling conveyor belt, these edifices must ultimately get destroyed at subduction zones. As a guyot or seamount progresses through a subduction zone, it will likely first experience a positive vertical deflection as it moves over the outer rise. This is because the lithosphere is assumed to behave as an elastic plate. Thus, just like when an elastic beam is bent, a small deflection in the opposite direction will occur just on the other side of the point of maximum flexure. While the lithosphere as a whole is considered to be elastic over long timescales, the upper portion of the plate experiencing the severe bending will behave brittlely. The underside of the plate at this bend experiences compression while the upper section is put under tension. As a guyot rides up over the outer rise, it may experience some deformation as the lithosphere which its built upon gets extended. Significant amounts of mass wasting likely occur along with the normal faults which develop with azimuths corresponding to the regional fracturing pattern. Much more severe faulting of the guyot occurs on the inner slope of the trench before it gets completely subducted [Lonsdale, 1986].

Given the association of guyot faulting with subduction zones, it is reasonable that tectonically-produced peaks should be expected on guyots which are approaching trenches. The northwesternmost reach of the Louisville Seamount Chain intersects the

Kermadec Trench at roughly 26.0°S. Thus, Guyot 26.0°S has the only guyot summit plain which exhibits clear faulting. The bathymetric map of Guyot 26.0°S, shown in Figure 13, displays several linear or slightly curved fault-scarps trending roughly north-south. These faults disrupt the summit plain so severely that the originally flat guyot morphology is no longer apparent. Instead there is a scattering of elongated peaks and ridges strewn across the surface which also trend roughly north-south. The large triangular peak on the northwest corner appears to have been tectonically uplifted relative to the central portion of the guyot. The steeper, small conical peak located on the southeast corner is more likely due to constructional volcanism, based on its morphology.

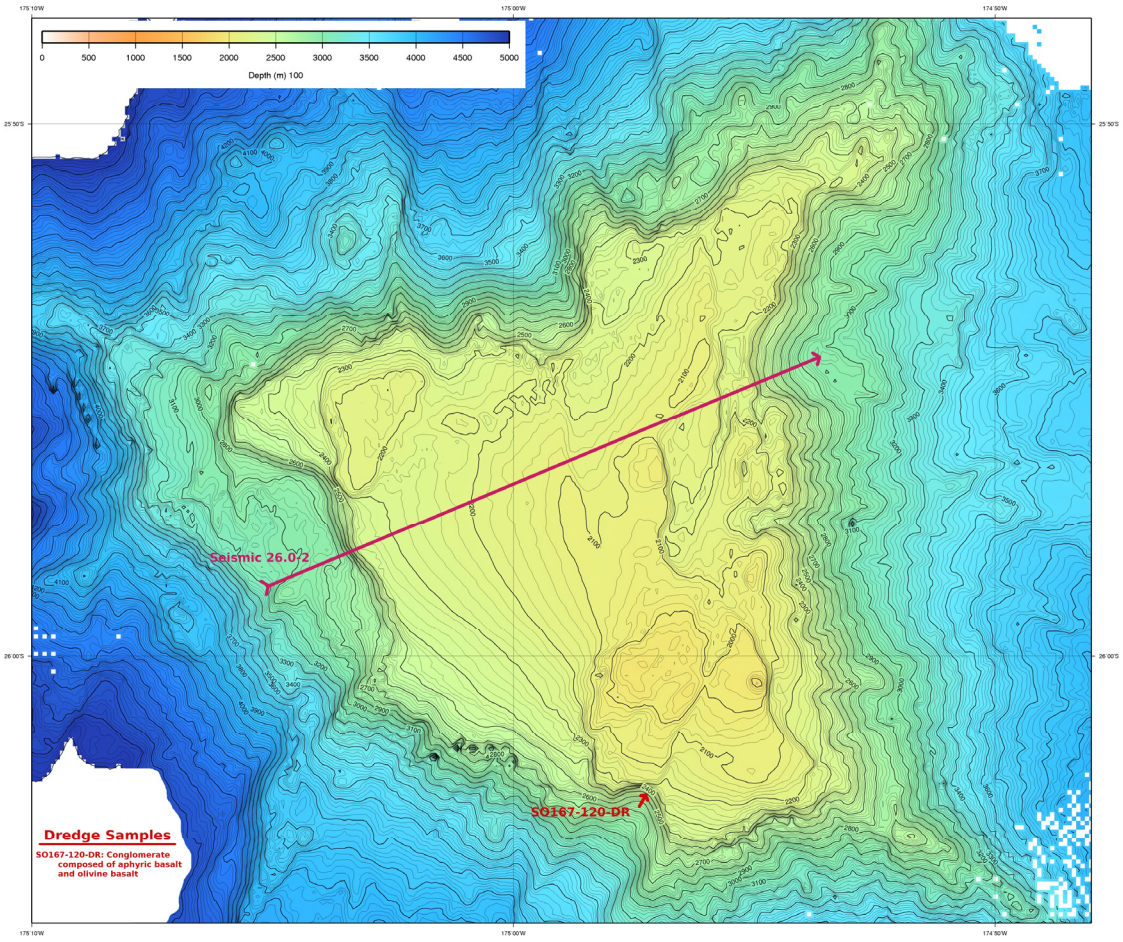

Figure 13: Bathymetric map of Guyot 26.0°S with seismic line and dredging site shown

Much of the faulting thus far appears to have taken place on the eastern side of the summit plain, but there also seems to be a large block that has been step-faulted from the western portion down into the trench. This large displacement can be seen on the left side of the seismic profile 26.0-2, included as Plate 6. Some of the smaller fault offsets are represented on the right side of the profile, but due to the orientation of the shiptrack there are prevalent side-echoes which make some of the tilted fault blocks overprint others. Also demonstrated in the MCS data, is the tilted nature of the original

guyot summit plain. In the process of moving up over the outer rise and then down into the inner slope of the trench, the summit plain of Guyot 26.0°S has been tilted roughly 2.5° to the west [Lonsdale, 1986]. After faulting had occurred, the current-trimmed dome of sediment overlying the summit plain was reworked to fill in low areas and smooth out the contours. It is not possible to clearly identify any fault planes or offset beds in MCS data due to the abundance of hyperbolas which appear because of side-echoes and steeply angled features.

3.3.5 Peaks of Biogenic Origin

Multibeam bathymetry data collected from Guyot 168.0°W (Plate 7) reveals a peculiar “guyot-on-guyot” [Lonsdale, 1986] structure that makes it stand out from the rest in the chain. A large, flattened platform (Figure 14) is built on the west-central portion of the guyot and is dissected into two unequal parts by a small north-south trending submarine valley. The small-scale contours shown in Figure 14 demonstrate that this structure had a unique and complex origin. Another flat-topped peak appears to the southeast of this main platform and has a similar summit depth. While not immediately relevant to the specific study of guyot summit plain peaks, the bathymetry on Plate 7 also reveals that a significant portion of the northeast summit plain has been down-faulted, perhaps due to circumferential faulting.

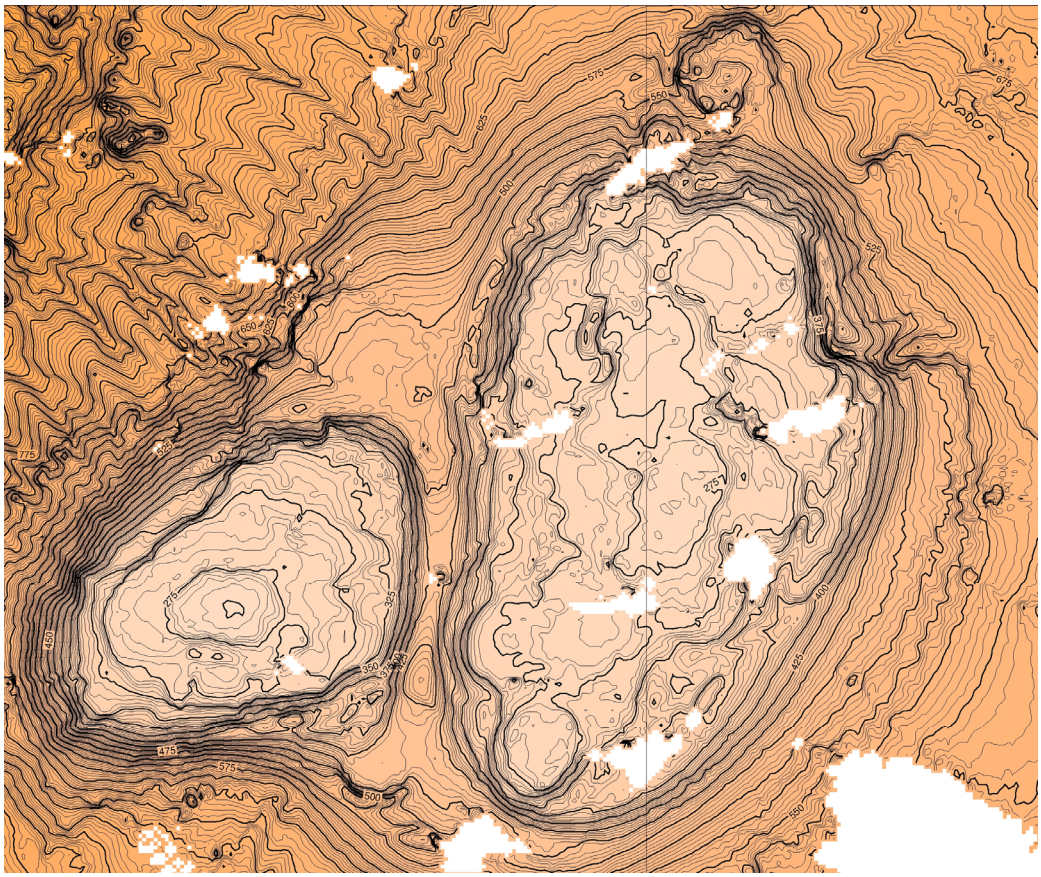

Figure 14: Small-scale map of the central platform on Guyot 168.0°W

The large main platform built upon Guyot 168.0°W was previously identified by Lonsdale [1998] and was suspected to be the result of posterosional volcanism, or perhaps represented a large erosional residual. Yet a dredge haul from this peak yielded a sample of nummulitic limestone, consisting primarily of the large benthic foraminifera *Paleonummulites pengaronensis*. Additional dredges were performed later during the AMAT02RR cruise on other sections of this main flattened peak which confirmed that the primary lithology composing (at least the outer portion of) this structure is in fact nummulitic limestone. The presence of lithified foram limestone on most of these

guyots is no major surprise since pelagic foram tests have been slowly raining down on these plateaus since submergence. But the presence of a limestone composed mainly of benthic foraminifera is less common for volcanic edifices originating at such high-latitudes.

MCS profiling performed on Guyot 168.0°W yields some of the most informative images of anywhere in the chain (Plate 8). The main guyot summit plain surface can be seen sloping gently outward toward its flanks beneath thick overlying sections of reflections which likely represent pelagic sediments and reworked carbonate sediments. The generally smooth erosional surface is interrupted in areas by more resistant plugs. These residual knobs form small regional basins, best exemplified on the right side of Plate 8, which are the first areas to be filled with subsequent sedimentation. Clearly identifiable, laterally-coherent reflections are abundant below the summit plain erosional surface and are interpreted to be an interval of extrusively erupted volcanic products. The large flattened peaks built above the summit plain are relatively uncommon and require a more complicated explanation.

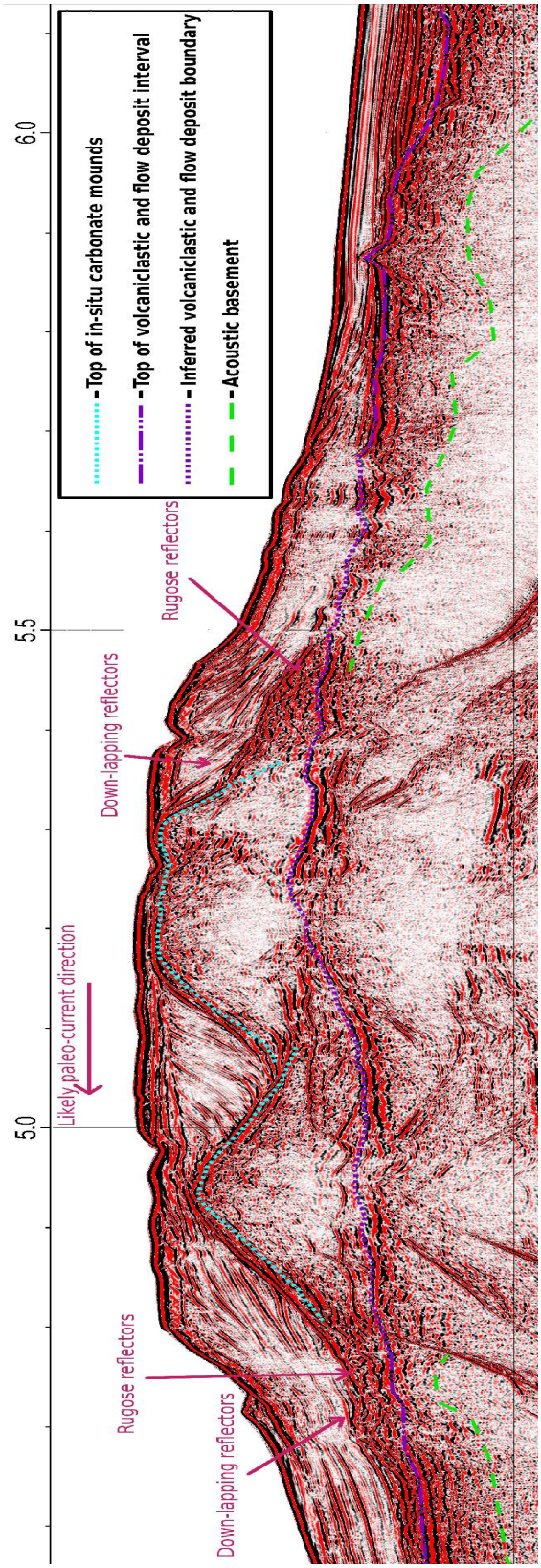

Figure 15: MCS data from Profile 168.0-1 on Guyot 168.0°W displaying the complex internal structure of the large, central carbonate platform

The internal structure of the large platform built on Guyot 168.0°W is rather well resolved in Figure 15. Two mounds, with limited internal reflections, appear to form the foundation for this structure with prograding sediment packages having filled the space in between and covering their outer slopes. The acoustic basement cannot be confidently identified beneath this central structure because the shallow water depth of this guyot causes the long-path multiple to arrive so soon that it interferes with primary reflections. Based on their high-amplitude tops, apparently high-amplitude base (blurred by multiple), reflection-free zones, and effective transmission of seismic energy through them, the structural mounds are interpreted to be relatively uniform nummulitic limestones. The down-lapping nature of the sediment beds indicates that the mound tops were likely sources of the reworked sediments and that there was a prevailing paleo-current from right to left for Figure 15. From the bathymetry data in Figure 14, it is possible to identify the tops of several other flattened carbonate mounds which act as the structural frame for the large platform that has been preserved. The platform also retains some evidence of slumping, preferential deposition, and drainage channels. The rugose reflections seen to either side of the mounds may represent reef-rubble which has broken off of the main reef. The strong bubble pulse multiple that is observed in the shallow subsurface across much of the profile shown on Plate 8 and Figure 15 is useful for indicating where hard rock is present at the surface of the guyot summit plain. It indicates that the upper surface of the large platform is well-lithified while the majority of the surrounding guyot summit plain is overlain by a significant thickness of unlithified sediment.

The transition from in-situ carbonate mounds, to reworked locally-deposited

carbonate sediments, to a relatively flat summit morphology provides evidence as to the conditions present during the later stages of carbonate-reef development. The inability to cement more sediments to the primary mound features indicates that there was an increase in hydrodynamic energy. Most likely, the carbonate mounds built themselves upward until they approached sea-level, at which point additional foraminiferal tests were washed off onto the flanks of the mounds, causing a more lateral pattern of growth. This scenario has been modeled by Kendall and Schlager [1981] during their analysis of the responses of isolated carbonate platforms to relative sea level change. Their model which best describes the conditions present at Guyot 168.0°W is when the growth potential of the interior begins to exceed the relative sea level rise. When this occurs, margin sedimentation catches up to sea level and progrades over the platform. If these conditions were sustained for long enough, the entire guyot summit plain would eventually be built up to sea level with carbonates.

Considering the carbonate platform was not ultimately able to spread across the entire guyot summit plain, there must be a reasonable explanation for why reef growth terminated. This is a complicated issue that studies concerning the development of drowned volcanic island edifices have dealt with in a variety of ways [Rougerie and Fagerstrom, 1994; Winterer et al., 1995]. The simplest answer often suggested is that relative sea level rise outpaced the carbonate reef growth rate. But this interpretation is quickly refuted by estimates of carbonate-reef growth rates which far surpass the largest subsidence rates yet observed. Another simple explanation might be that seafloor spreading has transported the edifices to high-latitudes where the tropical organisms cannot survive, but the Louisville guyots are actually moving toward the equator. One

popular interpretation for the death of such reefs is the exposure of them to low-oxygen, nutrient-rich, and/or turbid waters. This mechanism was chosen as the most-fitting for the guyots surveyed during ODP Legs 143/144 because they appear to have moved through the upwelling equatorial zone at about the same time that reef growth ceased [Winterer, 1998].

No apparent evidence exists to support abnormally fast subsidence or slow carbonate reef growth for Guyot 168.0°W, nor is there an associated event established in the literature which promoted regional, temporal upwelling. Rather, the most reasonable and simplest explanation for the cessation of carbonate reef growth is that the organisms responsible for producing the carbonate sediments disappeared. The persistence of the only confirmed fossil from Guyot 168.0°W, *Paleonummulites pengaronensis*, is quite limited in the sedimentary record. As discussed previously, the Eocene was a time of relatively high atmospheric and oceanic temperatures, but the end of the late Eocene is defined by an abrupt significant increase seen in d18O data, which represents a drastic cooling event [Bohaty and Zachos, 2003]. It is very likely that the temporarily high temperatures which allowed such large benthic foraminifera to thrive on this high-latitude guyot cooled so significantly that these organisms could no longer survive there.

The extinction of similar benthic foraminifera was not out of the ordinary for this time and region. Over the time period of mid-Eocene to Oligocene, there were numerous species of large benthic foraminifera which died off. Investigators have shown that benthic foraminiferal faunal changes occurring at this time happened in a stepwise manner. Three distinct periods of extinction are observed at about 46.7-44.6

Ma, 40-37 Ma, and 34-31.5 Ma. Each of these intervals are associated with unique faunal community changes, but the one most relevant to an assemblage containing *Paleonummulites pengaronensis,* appears to be the 34-31.5 Ma extinction period. This event has been interpreted as a response to the gradual cooling and increased corrosiveness of deep waters [Berggren and Prothero, 1992].

While Guyot 168.0°W displays the most apparent evidence of carbonate reef growth, it is not the only one interpreted to have experienced it. Considering that the benthic assemblage present at Guyot 168.0°W was likely capable of thriving at high-latitudes for millions of years, it seems likely that one or more of the neighboring guyots would also have been present near sea level and capable of sustaining communities of large benthic foraminifera. The multibeam bathymetry and MCS data for Guyot 168.6°W, located just northwest of Guyot 168.0°W, is shown on Plate 9. Both images demonstrate that the outer perimeter of the edifice is consistently shallower than the majority of the inner edifice. This is the sole example of this in the entire chain and can most reasonably be interpreted as an atoll with discontinuous perimeter carbonate mounds. It is likely that the carbonate reef on its summit emerged above sea level and had the central, lagoonal material removed by dissolution while leaving much of the perimeter reef intact [Winterer, 1998].

Reef emergence and the onset of subaerial erosion would require a significant relative lowering of sea level which cannot be confidently shown here, but is likely based on the drastic increase in the $d^{18}O$ record corresponding to the Eocene-Oligocene boundary (~33.5 Ma) [Kennet and Exon, 2004]. Also, small-scale contours seen on the carbonate platform could be reasonably attributed to karst topography.

Another example from the chain which appears to have experienced reef growth, or at least abnormally high amounts of sedimentation, is Guyot 167.4°W, but the data coverage is extremely poor. There is no MCS data and the multibeam bathymetry data does not give full coverage of the summit plain or display any obvious peaks. The best data collected from this guyot which can contribute to an interpretation is the 3.5 kHz Knudsen data (Plate 10). In the Knudsen profile, there are three peaks of unknown origin buried by up to 70 m of what appears to be sediment. Other than Guyot 168.0°W, this guyot has the greatest thickness of posterosional sediments found on the chain. Reflections within the sediment beds appear to correlate across the entire guyot, but are separated by the peaks rising from acoustic basement. These peaks have clearly influenced the pattern of sedimentation, but no distinct onlapping or downlapping reflections can be identified at this resolution. The interpretation extended here for how this scenario of fully buried peaks could occur, especially considering the proximity of 168.0°W, is rapid carbonate sediment deposition in a shallow-water environment which ceased only once the organisms responsible went extinct or were no longer present in the photic zone. This is quite reasonable given the estimated age of 39-40 Ma for the guyot [Lonsdale, 1988]. This would allow for several millions of years of erosion to flatten the summit plane, followed by several millions of years of carbonate sediment production by large, benthic, carbonate-secreting organisms before extinction or removal from the photic zone. Alternatively, a drastic increase in pelagic sediment input could have occurred due to the setting up of the Southern Ocean system at the end of the Eocene, which increased the amount of upwelling and primary production in the region [Kennet and Exon, 2004]. The interpretation that carbonates compose the upper

surface of Guyot 167.4°W is further supported by the tentative identification of a sinkhole in the cruise log which corresponds to the dip seen at the center of the guyot summit plain.

3.3.5 Timing of Carbonate Reefs on Louisville Guyots

Radiometric dating of basalt samples collected from Guyot 168.0°W suggest that the main shield-building stage of volcanism was nearing completion about 45-46 Ma [Lonsdale, 1988; Koppers, et al., 2004]. It is rather difficult to estimate the amount of time the guyot must have spent at sea level experiencing littoral erosion, but it is possible to get an idea of how long it would take the summit plain to move through the photic zone, which is actually the time interval of interest here. By plotting guyot shelf-break depths versus the square root of estimated ages for these guyots, Lonsdale [1988] was able to develop an equation which describes the average rate of subsidence of Louisville guyots through time:

$$z = 248((t)^{1/2} - (2.4)^{1/2})$$

The maximum depth of the photic zone varies greatly depending on the regional environment, but considering the isolation of the Louisville Seamount Chain from terrestrial sediment inputs and the low primary productivity in the overlying water-column, it is reasonable to estimate a maximum photic depth of up to 150 m [Langer and Hottinger, 2000; Davies et al., 1972]. Assuming that the guyot summit slope-break marks the level at which erosion began on the emerged volcanic island, the equation above can be used with a z-value of 150 m to estimate how long it took for the outer perimeter of the guyot to subside below the photic zone. This method provides an

estimate of 4.6 million years for the outer guyot perimeter to move from sea level to 150 m below sea level. For most large guyots, at least some amount of relief (up to hundreds of meters) is preserved on the summit plains, which means that it would take even longer for the central portions to reach that same depth of 150 m. Using the method and assumptions described above, a reasonable estimate for the time interval that the summit plain of Guyot 168.0°W spent in the photic zone is from about 38-45 Ma.

Limestone samples dredged from the large flattened peak on Guyot 168.0°W were at least partially composed of *Paleonummulites pengaronensis*, based on a small sample sent for microfossil identification. This specific type of large benthic foraminifera has been identified in a number of assemblages from Eocene-age sediments in the Indo-Australian region. The first appearance of this specific taxa is estimated to be around 40.5 Ma, and they are thought to have gone extinct by about 32 Ma [Renema, 2002]. Therefore, *Paleonummulites pengaronensis* (and likely similar large benthic foraminifera as well) was most likely an extant species around the same time that the summit plain of Guyot 168.0°W was moving through the lower photic zone.

The timing of events seems to support the interpretation originally extended for the onset and termination of carbonate reef growth quite well; however, there is one major complication with this explanation. If the carbonate reef on Guyot 168.0°W ceased growing around 32 Ma, and was therefore at or near sea level at this time, it should have subsided much deeper below sea level in the time since. According to the Louisville guyot subsidence equation used in the previous section, the vertical change in

depth that the guyot should have experienced in 32 million years is roughly 1000 m. Yet the current depth to the shallowest part of the carbonate platform is only about 250 m! Based on this depth, it would be estimated to have been at or near sea level as recently as 6-10 Ma. Potential explanations for this large discrepancy might be: 1) Guyot 168.0°W has experienced some form of thermal rejuvenation since 32 Ma, likely from riding over a thermal anomaly; 2) this specific region somehow experienced abnormally slow subsidence for the given time interval; or 3) the benthic assemblage present at the guyot surface was able to survive beyond the estimated 32 Ma extinction date at this unique location. Of these, the first two explanations are the most compatible with the observed data. If the 1300 m depth originally chosen as the guyot slope break is reinterpreted to be due to circumferential faulting and therefore not representative of the paleo-sea level, a newly designated slope break of about 900 m would be appropriate. This would mean that the entire edifice is anomalously shallow, thus adding credence to the thermal anomaly explanation. Alternatively, if the Wishbone Scarp, which Guyot 168.0°W was built upon, is assumed to represent a fracture zone transverse ridge, then it should be expected to have subsided more slowly than the other guyots. Note that if this explanation of slow subsidence is favored, then the use of the generalized Louisville guyot subsidence equation in the previous section is no longer valid.

4

Conclusions

The preserved morphologies of the Louisville guyots provide valuable evidence of the dominant processes affecting them around the time of marine planation as well as any significant events occurring after submergence. The four types of peaks in this study were primarily interpreted based on the characteristic geophysical signals they return, which reflect the conditions which they formed under. A summary of the observed geophysical data, collected lithologies, and the final peak origin interpretations for those guyots with sufficient data coverage are shown in a table on Plate 2.

The most easily attributable peaks on a guyot in the Louisville Seamount Chain are those of Guyot 26.0°S. The coincidence of this edifice with the Tonga-Kermadec subduction zone and the presence of linear ridges with approximately the same azimuth as the trench and nearby lithospheric faulting pattern are strong evidence that these features are of tectonic origin. This tectonic activity has overprinted the geomorphology previously inherited upon submergence and therefore is not useful for whole-chain interpretation. The other three types of peaks, however, do likely provide constraints on the timing and location of certain processes. The spatial, and therefore also roughly temporal, distribution of Louisville guyots and seamounts is shown in Figure 16 with the interpreted origins of the summit plain peaks shown. Those without obvious peaks are represented solely by their average break in slope depths.

Figure 16: Graph showing relative positions of guyots with peaks of each type of origin

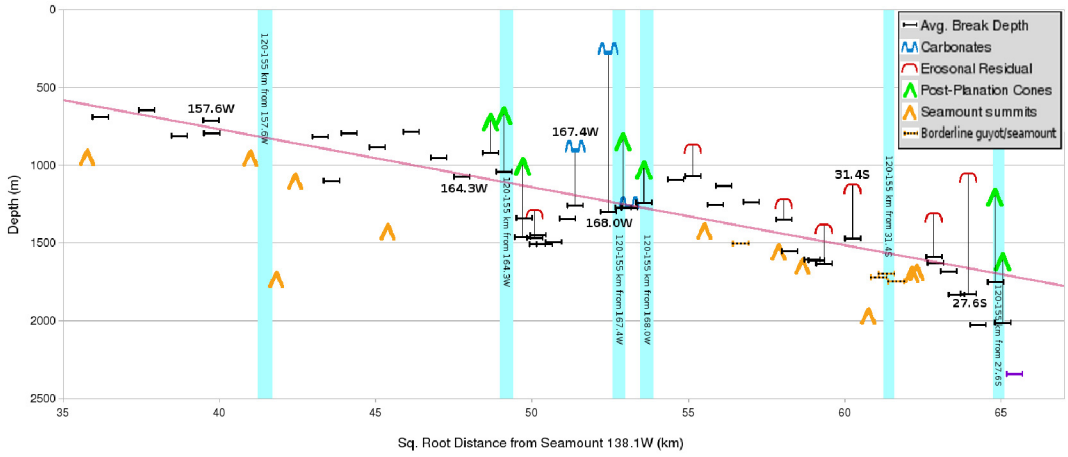

There are several relationships worth noting in this figure, which follows from a similar graph in Lonsdale [1988]. The regression line representing the Louisville guyot subsidence equation, $z=248((t)^{1/2}- (2.4)^{1/2})$, clearly follows the general trend of measured guyot slope breaks. This supports the concept that guyots record the regional sea level at the time of submergence, then subside along with the underlying lithosphere as a function of the square-root of time. The lone purple symbol on the far right side of the figure represents the slope break depth for Guyot 26.0°S, and it diverges significantly from the general trend because of the influence of the nearby trench. The only guyots with carbonate-reefs present on their summit plains are located toward the middle of the chain. This simply demonstrates that these were the only summits within the photic zone during the limited time interval in which large benthic foraminifera were capable of thriving at high-latitudes. Guyots exhibiting erosional residual peaks are somewhat more widespread, but still appear to be more prevalent on the older

section of the chain. This may be due to a combination of generally smaller edifices being built over time, better data coverage of the older portion, and perhaps an increase in sediment supply once the Southern Ocean circulation system developed [Kennet and Exon, 2004]. The six largest guyots in the chain are labeled on Figure 16 and have associated light blue zones which represent a distance of 120-155 km in the direction of the next oldest edifices. The observation that post-planation volcanism seems to occur on neighboring guyots within a roughly 120-155 km interval follows from a similar observation by Clague et al. [1989]. They found that posterosional volcanism in the Hawaiian-Emperor Chain tended to be preferentially located about 190 km ± 30 km away from the next large shield volcano being built. It should be expected that the characteristic distance for the appearance of rejuvenated volcanism would vary from chain to chain, due to its likely dependence on regional flexural rigidity. As shown, the 120-155 km estimate for the Louisville Seamount Chain holds up well for Guyots 167.4°W, 168.0°W, and 27.6°S. There are two edifices with post-planation volcanic cones located just outside of the light blue interval associated with 164.3°W. This suggests that the area of influence may have been somewhat larger here for some reason, assuming this distance is in fact related to the actual mechanism allowing secondary volcanism. The lack of posterosional cones in the 120-155 km intervals for Guyots 154.3°W and 31.4°S is to be expected since there were not any established guyot summit plains available to erupt upon. Rather, the upper summits of the volcanic edifices which never reached sea level in and near those two light blue intervals could possibly have been formed by secondary eruptions, as opposed to while still located over the primary magma source.

One of the primary components of this study is the identification of guyots with constructional volcanic cones on their summit plains for the purpose of inferring possible temporal and spatial correlations for rejuvenated volcanism. The spatial relationship of 120-155 km discussed above does appear to support the concept that post-planation volcanism on guyots is triggered by the building of large shield volcanoes a specific distance away. As for temporal observations, minimum time intervals between truncation and secondary volcanism can be estimated using the Louisville guyot subsidence rate and by assuming that the pointed summits indicate that sea level was not reached. Such calculations were done here for the guyot summit plain peaks on Guyots 169.0°W, 165.4°W, 165.7°W, and the potentially transitional peaks on Guyot 26.6°W. The minimum elapsed time intervals calculated here are: 6 Ma, 7.6 Ma, 8 Ma, and 4.5 Ma, respectively. These values fall right in the middle of the estimated 1-10 million year hiatus estimated by Staudigel and Clague [2010].

Those edifices with erosional residuals clearly disrupting the flat summit plain potentially indicate one or a combination of the following conditions: 1) the level at which the volcanic island was planed flat was low enough that primary intrusive conduits or plugs have been exhumed; 2) the guyot was located in an environment where subaerial erosion rates were relatively low; or 3) the guyots experienced a period of abnormally fast subsidence which allowed certain portions of the summit plain to escape prolonged exposure to littoral erosion. Observations from geophysical data indicate that these are most likely resistant intrusive structures which have been uncovered by differential erosion.

The presence of shallow-water carbonates on the Louisville guyots effectively

adds a great deal of information about the physical conditions present at these edifices as they were subsiding, as well as providing time constraints. It is interpreted in this study that the abnormally high seawater temperatures associated with the warm Eocene allowed certain species of large, benthic foraminifera to thrive at high-latitudes. Dredged samples indicate that foraminiferal tests made by benthic organism assemblages are likely primary components of the carbonate platform on Guyot 168.0°W. Based on the estimated period in which *Paleonummulites pengaronensis,* the only confirmed fossil from the Guyot 168.0°W, was an extant species, a straightforward explanation for the timing of reef growth initiation and termination can be developed. Carbonate reef growth may have started around 38-40 Ma while the summit plain of Guyot 168.0°W was in the lower photic zone. The platform then rapidly grew up to sea level at which point it was forced to grow outward as opposed to upward. The drastic ocean cooling that occurred at the start of the Oligocene provides a reasonable mechanism for both the termination of reef growth here as well as the extinction of the large benthic foraminifera assemblage present at the guyot. The complication stemming from the unexpectedly shallow depth of this platform in modern times is most likely explained by abnormally slow subsidence of Guyot 168.0°W due to its location on what is believed to be a fracture zone transverse ridge, known as Wishbone Scarp.

The geophysical data and interpretations presented in this study establish the four distinct origins for the guyot summit plain peaks found in the Louisville Seamount Chain. Without the aid of deep-sea drilling data for groundtruthing, it is difficult to accurately predict what the nature of such features might be, but by applying geomorphological concepts to structures observed in high-resolution geophysical data it

is possible to make reasonably confident interpretations. The presence of peaks on guyot summit plains and their specific origins are tremendously useful for volcanic island chain studies since they preserve a record of the conditions existing at each edifice as it is being planed flat at sea level and submerging. The constraints and observations provided by this study are intended to contribute to the development of a complete evolutionary model for the Louisville Seamount Chain. Even though this study focused specifically on a single oceanic island trail, the methods were developed such that they can be extended to other guyot trails with comparable data coverage.

Appendix

Plate 1 – Louisville Guyot Index Map

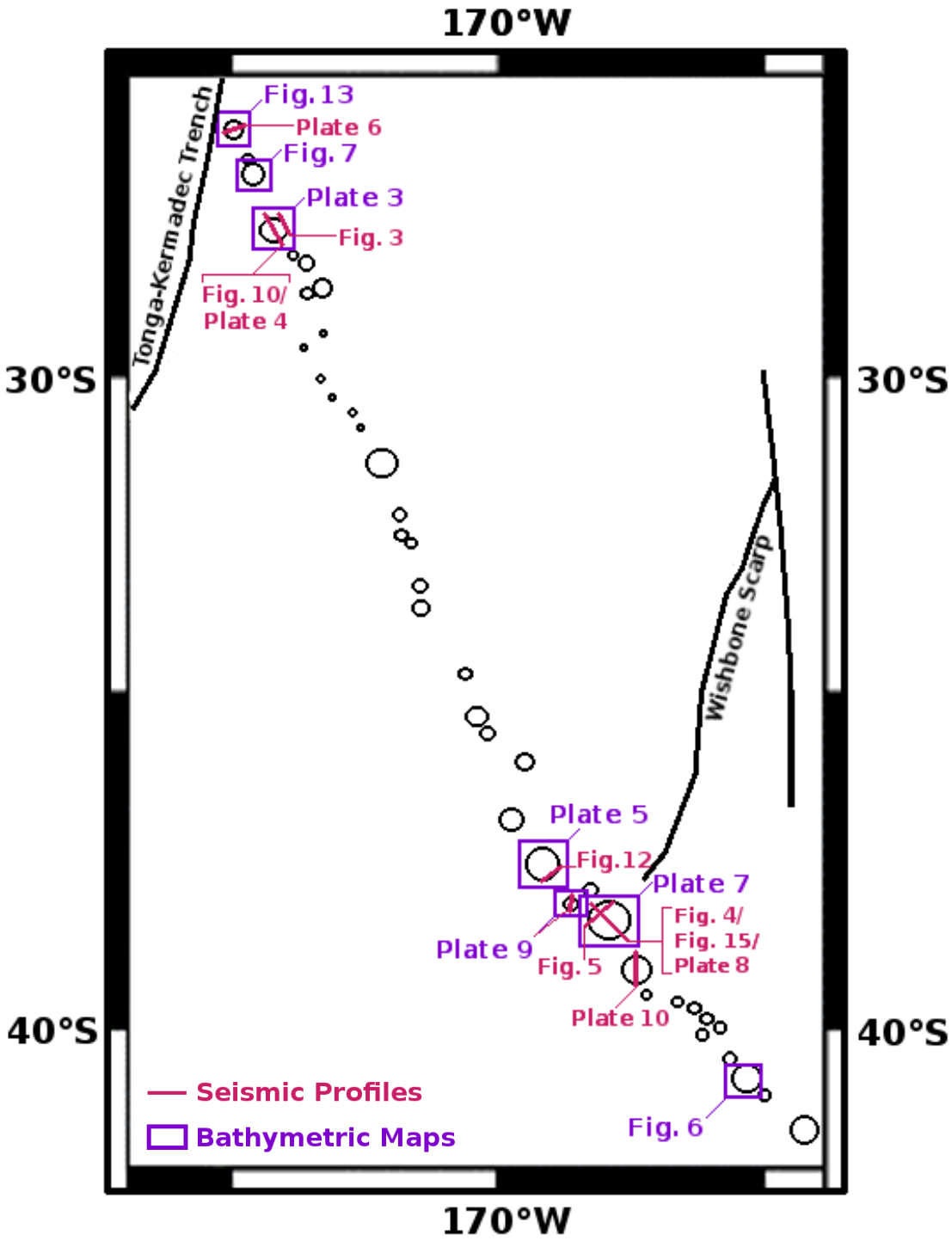

Plate 2

Primary observations on which interpretations are based								
Guyot	Bathymetry Data	Seismic Data	Dredge Samples		Avg. Flank Slope of Peaks	Max. Flank Slope of Peaks	Other Observations	Final Interpretation
			Sample ID	Lithology				
26.0°S	Linear ridges with relatively uniform azimuths; fault expressions	Originally horizontal bedding is uniformly tilted; offsets across faults cannot be seen due to oblique crossings and side-echoes	SO167-117-DR; SO167-120-DR	Oxidized, red pyroxene basalt (subaerial lava); conglomerate with various lithologies (paleo-beach deposit)	14.5° (constr.)	20° (constr.)	Presently located on the outer rise of a subduction zone	**Tectonic Origin** with a solitary **Constructional Volcanic peak**
26.5°S	Several steep, conical peaks over main core and around perimeter	No erosional surface can be identified; prevalent side-echoes from out-of-plane peaks	SO167-134-DR	Weathered olivine-plagioclase basalt	17°-19°	23°-28°	Possible fault expression on the western side	**Constructional Volcanic Origin**
26.6°S	Numerous semi-conical peaks spread across entire summit plain	Thick succession of sedimentary beds above hard rock surface	SO167-135-DR	Pieces of dense, aphyric basalt ranging from weakly to deeply weathered	5°-12° (w/ erosion) 15°-18° (constr. only)	15°-18° (w/ erosion) 23°-24° (constr. only)	Evidence of erosion near the summits of some peaks	**Constructional Volcanic Origin** with erosional influence
27.6°S	Several peaks, the majority of which are centrally located; broad bulge	Central peaks appear to be conformable with acoustic basement	SO167-139,140,141-DR	Breccias and conglomerates composed of phyric and aphyric basalts (paleo-beach)	4°-14°	12°-18°	Channels have developed around the more erosionally resistant peaks	**Erosional Volcanic Origin**
28.6°S	Two broad peaks over the main cores of the coalesced guyots, few perimeter peaks	Peaks appear to be conformable with acoustic basement; no overlying volcaniclastics	SO167-147-DR	Breccias with class of olivine basalt and aphyric basalt (paleo-beach)	5°-15° (erosional) 22° (constr.)	12°-19° (erosional) 30° (constr.)	Western perimeter peak has much steeper flanks and is likely constructional	**Erosional Volcanic Origin** with perimeter peak of **Constructional Volcanic Origin**
31.4°S	No sharp peaks, but several broad bulges may represent remnants of resistant cores	Erosionally-resistant axis with thickening section of volcaniclastics toward edges	SO167-149-DR; SO167-152-DR	Weathered, non-vesicular aphyric basalt; non-vesicular olivine basalt	N/A	N/A	Erosional channels have developed across the guyot separating three intrusive cores	**Erosional Volcanic Origin**
169.0°W	Two guyot centers with low relief connected by a flattened NW-SE trending ridge; irregular, sharp peak present on SW corner	Erosionally-resistant axis with thickening section of volcaniclastics toward edges; regionally thicker sediments near SW peak	SO167-164-172-DR	Wide range of breccias and lava types with variable weathering	3° (erosional) 12° (constr.)	15° (erosional) 22° (constr.)	Channels have developed around the large knob on the northern section	**Erosional Volcanic Origin** with a solitary **Constructional Volcanic peak** on the SW corner of the southern section
168.6°W	Peaks and ridges line the outer perimeter, often separated by large scarps	Perimeter mounds perched on guyot summit plain edges; may be mound in center too	AMAT02-D-10	Aphyric basalt, pillow basalt, and volcaniclastic breccia with carbonaceous cement	3°-9°	8°-13°	Only guyot in chain with perimeter generally shallower than its center	**Biogenic Origin**
168.3°W	Relatively low-relief over most of the guyot with an angular peak on the northern corner	Erosionally-resistant center with a thickening section of volcaniclastics toward edges	AMAT02-D-7	Coarse-grained phyric vesicular basalt; breccia with volcaniclastic matrix and various basalts	16°	30°	Some drainage features are observed, but not around northern peak	**Constructional Volcanic peak** on northern corner
168.0°W	Very large guyot with flattened mounds on the west-central portion, a down-faulted NE perimeter, and a scattering of smaller peaks primarily on the western side	Platforms above the guyot summit plain allow seismic energy to penetrate to acoustic basement; sediment beds and ruble associated with these platforms thin outward	AMAT02-D-8; AMAT02-D-9; MRTN-02D	Calcareous sediment and corals; Paleonummulitic limestone; Paleonummulitic limestone	2°-10° (biogenic) 16°-21° (constr.)	13°-17° (biogenic) 18°-28° (constr.)	Erosional channels on NW portion cannot penetrate deeper than hard rock layer associated with bubble pulse multiple	**Biogenic Origin** with smaller peaks of **Constructional Volcanic Origin**
***167.4°W**	Poor data coverage obscures bathymetric expression of peaks (if there are any)	Knudsen data indicates at least two buried peaks above the guyot summit plain	AMAT02-D-13; AMAT02-D-14	Breccias and conglomerates composed of basalt and limestone fragments (forams and shells) in a carbonaceous cement	N/A	N/A	Deposition around former peaks appears to have been influenced by regionally produced currents	Guyot summit is of **Biogenic Origin**
***165.7°W**	Line of narrow, conical peaks trending N-NE	Knudsen data is of limited use here; only thin lenses of sediment are imaged	AMAT02-D-18,19,20	Volcaniclastic microbreccias; aphyric basalts; phyric basalts	15°-19°	21°-31°	North-central peak appears to be cratered	**Constructional Volcanic Origin**
***165.4°W**	Numerous conical peaks, the majority of which align in a N-NE trend	Relatively thick sections of sediment can be seen adjacent to peaks	AMAT02-D-21,22,23	Altered phyric basalts; volcaniclastic breccias; poorly-indurated foram limestone	15°-23°	21°-31°	Drainage pattern indicates a broad eroded plutonic core composing SE rift arm	**Constructional Volcanic Origin**

*3.5kHz Knudsen Data Only

Plate 3 – Bathymetric Map of Guyot 27.6°S

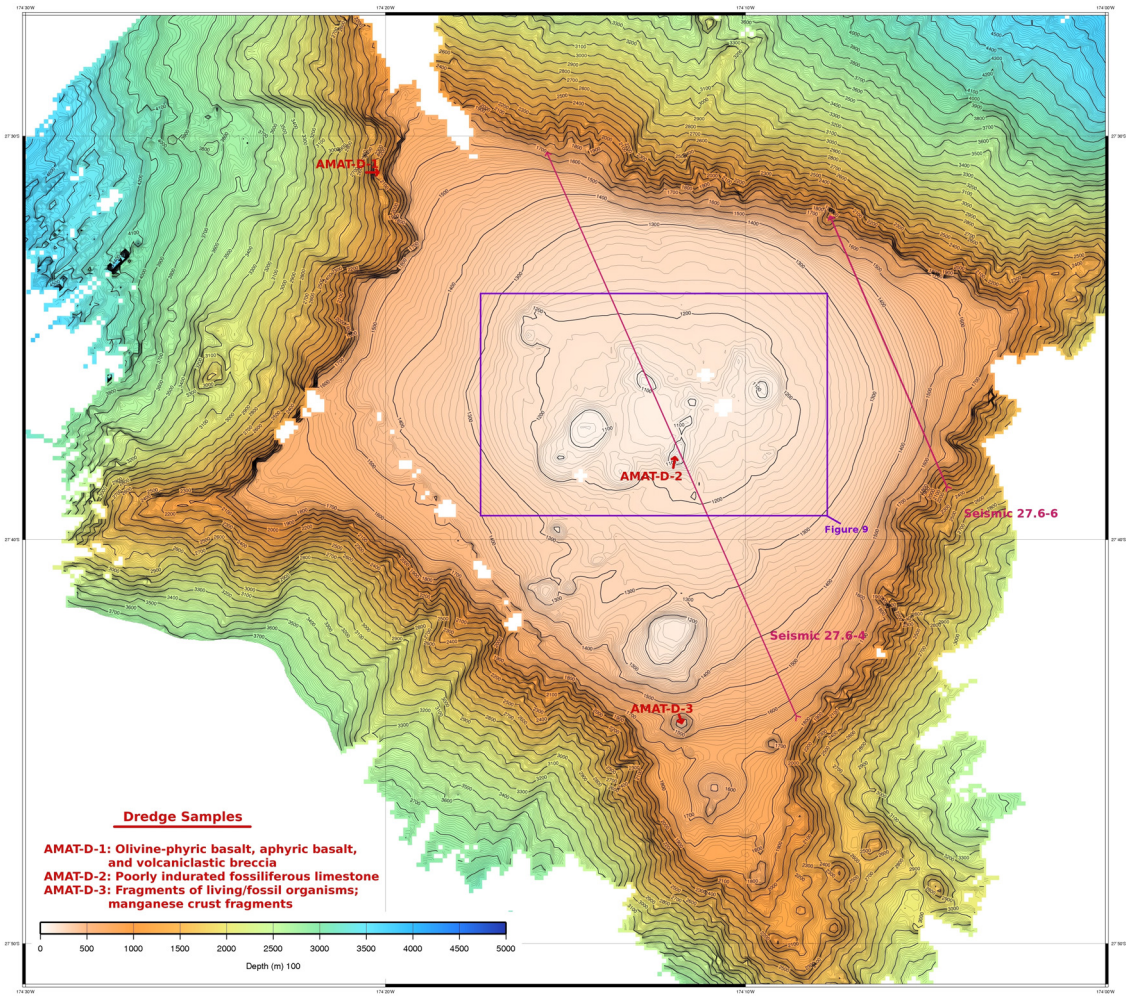

Plate 4 – Seismic line 27.6-4

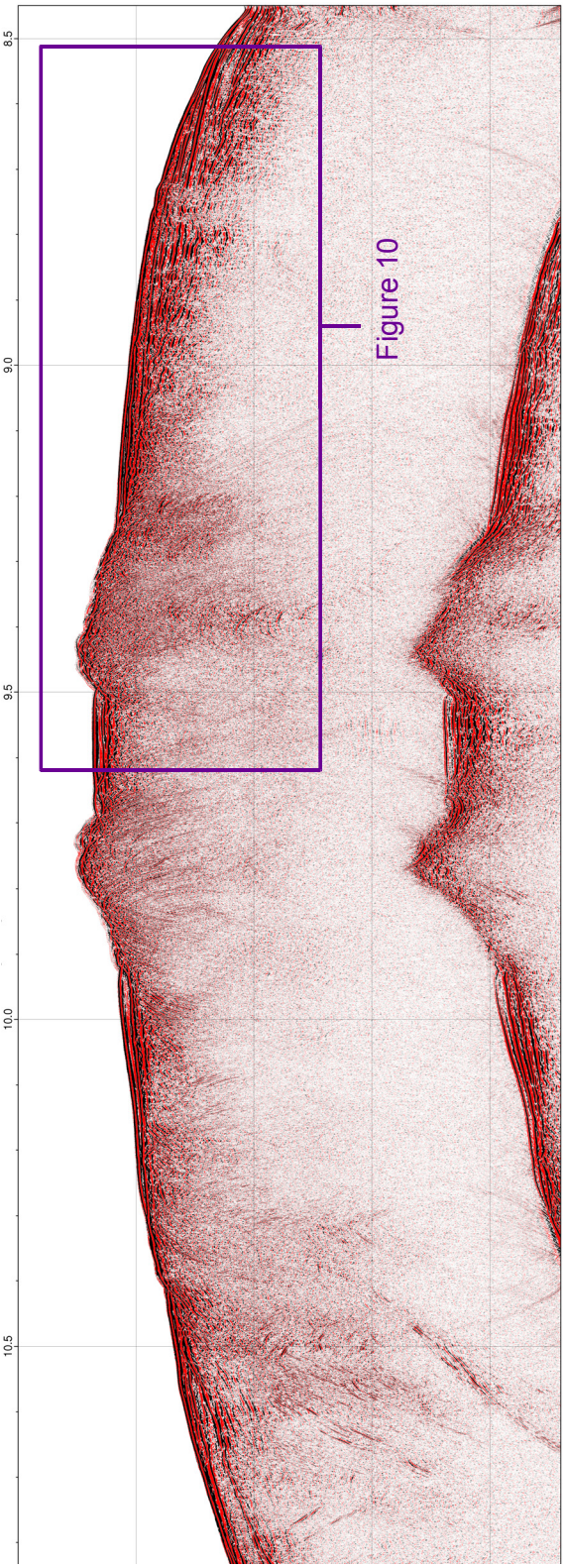

Plate 5 – Bathymetric Map of Guyot 169.0°W

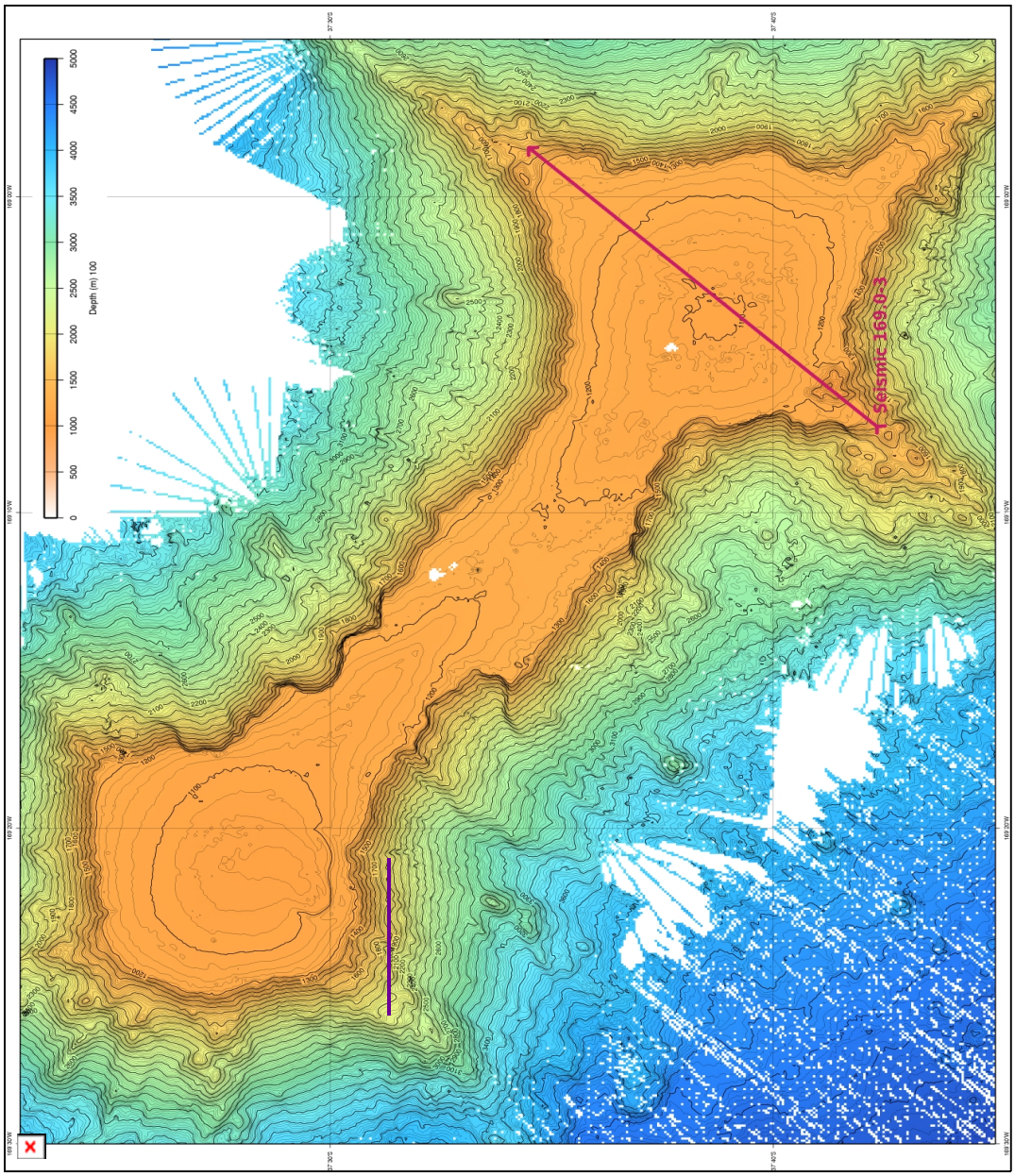

Plate 6 – Seismic line 26.0-2

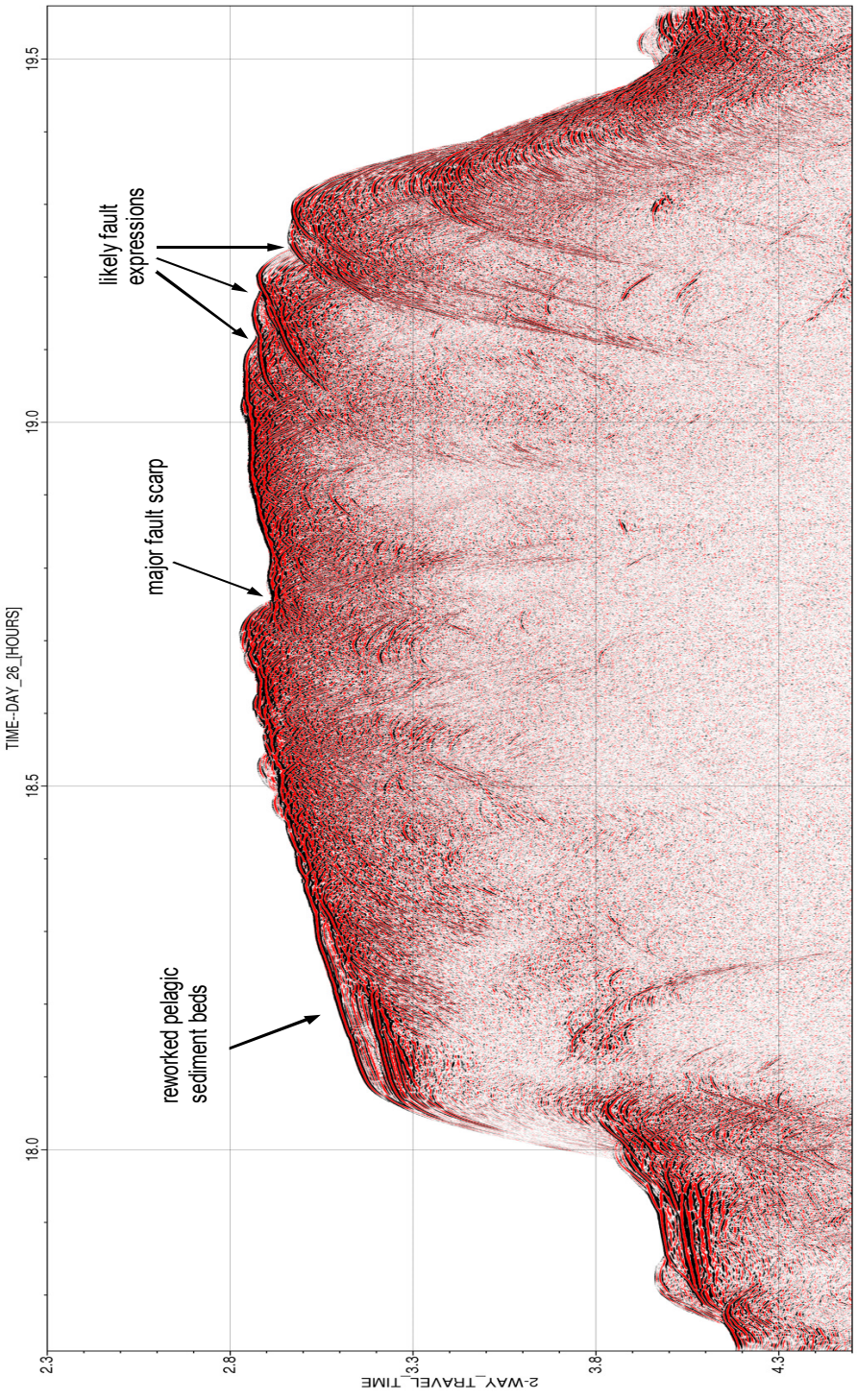

Plate 7 – Bathymetric Map of Guyot 168.0°W

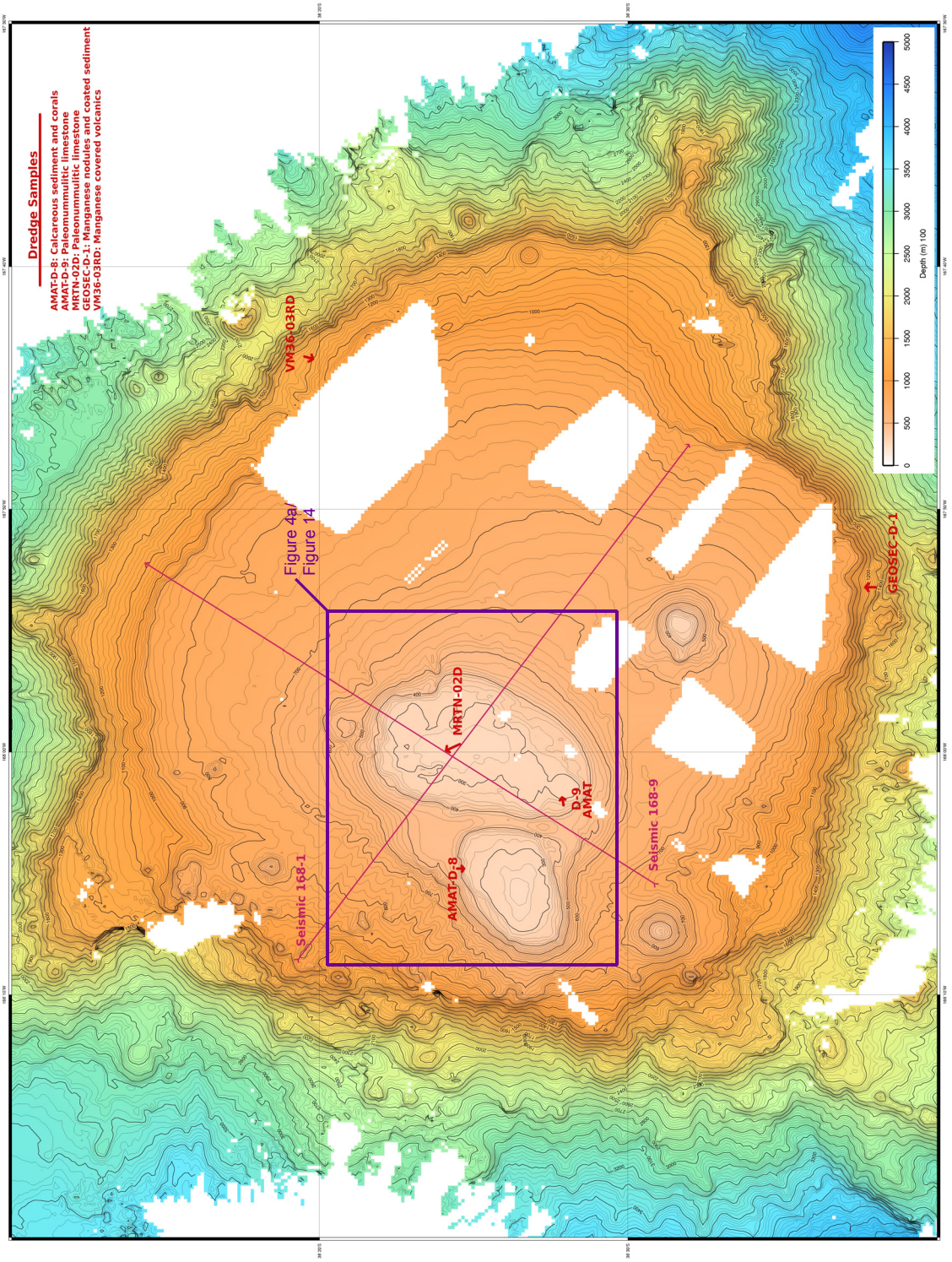

Plate 8 – Seismic line 168.0-1

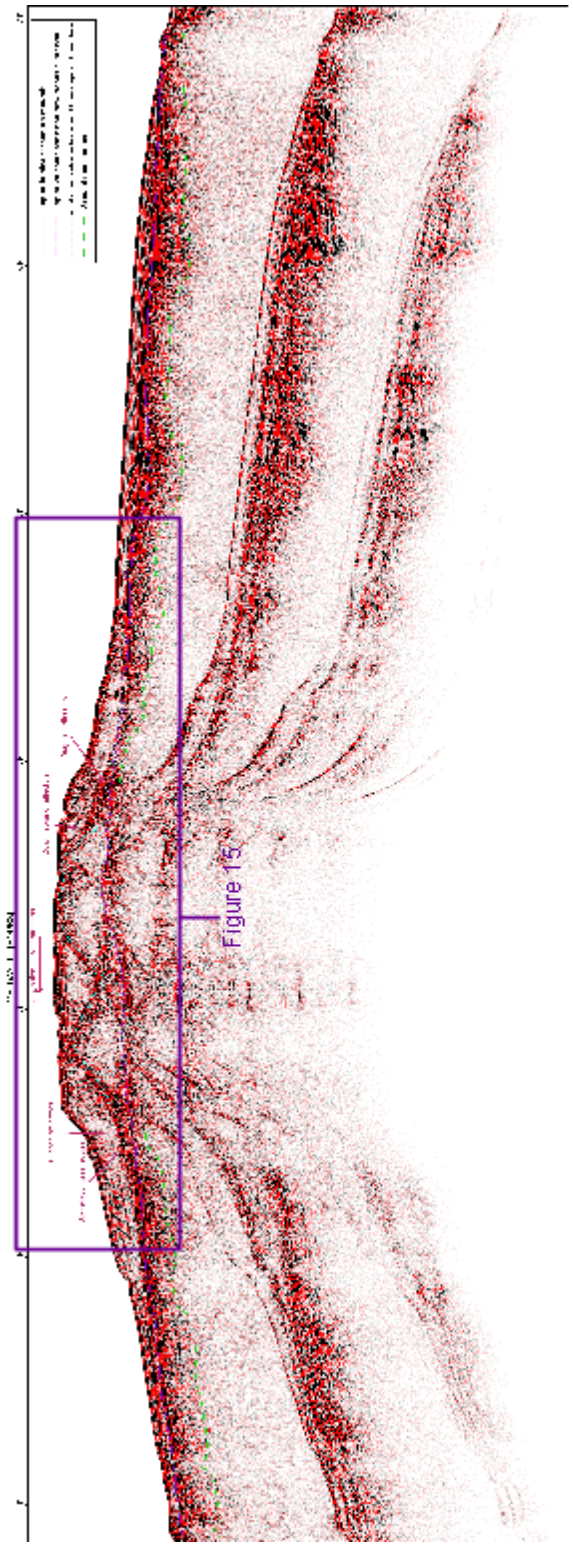

Plate 9 – Bathymetry and seismic data from Guyot 168.6°W

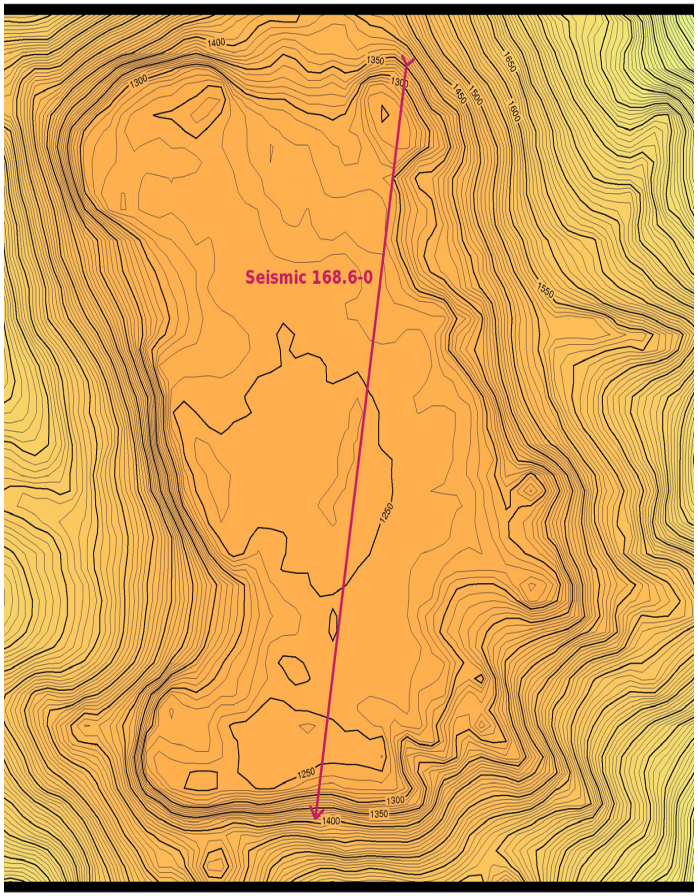

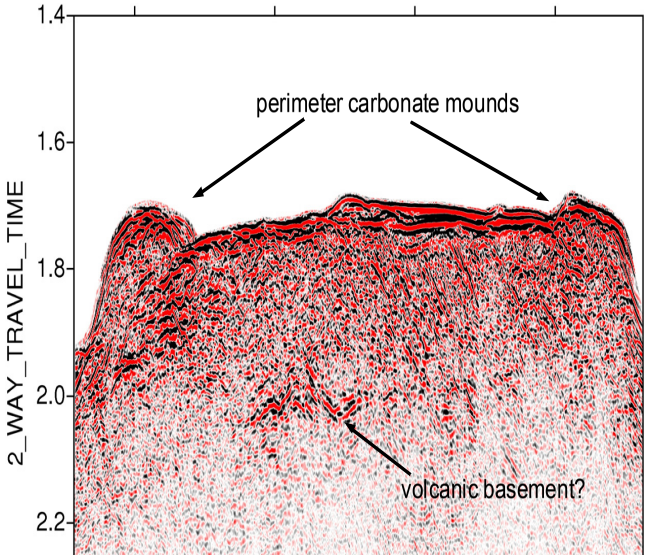

Seismic line 168.6-0

Plate 10 – 3.5 kHz CHIRP profile from Guyot 167.4°W

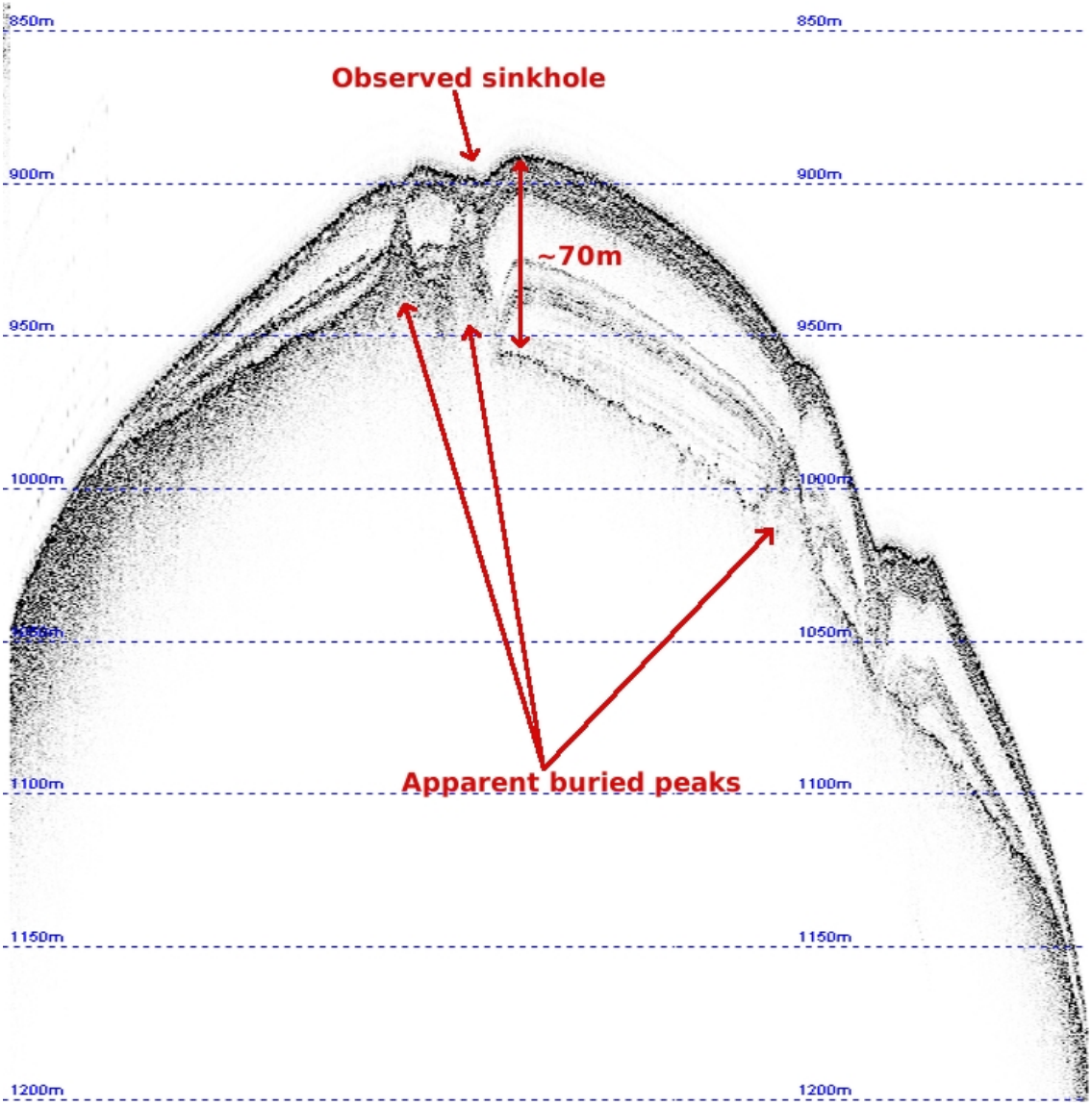

REFERENCES

Anstey, N.A., 1977. Seismic Interpretation: the Physical Aspects. Boston, MA: International Human Resources Development. Print.

Barone, A.M., Ryan, W.B.F., 1987. Morphology from subaerial erosion of a Mediterranean seamount. *Marine Geology*, 74, p. 159-172.

Becker, J. J., D. T. Sandwell, W. H. F. Smith, J. Braud, B. Binder, J. Depner, D. Fabre, J. Factor, S. Ingalls, S-H. Kim, R. Ladner, K. Marks, S. Nelson, A. Pharaoh, R. Trimmer, J. Von Rosenberg, G. Wallace, P. Weatherall., 2009. Global Bathymetry and Elevation Data at 30 Arc Seconds Resolution: SRTM30_PLUS, *Marine Geodesy*, 32:4, pg. 355-371.

Bergersen, D.D., 1995. Physiography and architecture of Marshall Islands guyots drilled during Leg 144: Geophysical constraints on platform development. in Haggerty, J.A., Premoli Silva, I., Rack, F., McNutt, M.K. (Eds.), 1995. *Proceedings of the Ocean Drilling Program, Scientific Results*. Vol. 144, p. 561-583.

Berggren, W.A., Prothero, D.R., 1992. Eocene-Oligocene Climatic and Biotic Evolution. Princeton, NJ: Princeton UP. Print.

Bohaty, S.M., Zachos, J.C., 2003. Significant Southern Ocean warming event in the late middle Eocene. *Geology*, Vol. 31, No. 11, p. 1017-1020.

Bonatti, E., Harrison, C.G.A., 1988. Eruption styles of basalt in oceanic spreading ridges and seamounts: Effect of magma temperature and viscosity. *Journal of Geophysical Research*, Vol. 93, No. B4, p. 2967-2980.

British Antarctic Survey, 2008. Web resource. Accessed June 10, 2010. <www.antarctica.ac.uk/.../em120_multibeam_swathbathymetry_echo_sounder.pdf>

Clague, D.A., Dalrymple,G.B., Wright, T.L., Klein, R.Y. Koranagi, Decker, R.W., Thomas, D.M., 1989. Chapter 12: The Hawaiian-Emperor Chain in Winterer, E.L., Hussong, D.M., Decker, R.W., eds. Tectonics, Geochronology, and Origin of the Hawaiian-Emperor Volcanic Chain. The Geology of North America, Volume N. The Eastern Pacific Ocean and Hawaii. p.5-40.

Contreras-Reyes, E., Grevemeyer, I., Watts, A.B., Planert, L., Flueh, E.R., Peirce, C., 2010. Crustal intrusion beneath the Louisville hotspot track. *Earth and Planetary Science Letters*, 289, p. 323-333.

Cotton, C.A., 1952. Volcanoes as Landscape Forms. Christchurch, NZ: Whitcombe and Tombs Ltd. Print.

Cowen, J.P., Giovannoni, S.J., Kenig, F., Johnson, H.P., Butterfield, D., Rappe, M.S., Hutnak, M., Lam, P., 2003. Fluids from aging ocean crust that support microbial life. *Science*. Vol. 299, p. 120-123.

Davies, T.A., Wilde, P., Clague, D.A., 1972. Koko seamount: a major guyot at the southern end of the Emperor seamounts. *Marine Geology*, 13, p. 311-321.

Fontaine, J.M., Cussey, R., Lacaze, J., Lanaud, R., Yapaudjian, L., 1987. Seismic Interpretation of Carbonate Depostional Environments. *AAPG Bulletin*, v. 71, No. 3, pg. 281-297.

Harris, R.N., Fisher, A.T., Chapman, D.S., 2004. Fluid flow through seamounts and implications for global mass fluxes. *Geology*, 32, p. 725-728.

Hess, H.H., 1946. Drowned ancient islands of the Pacific Basin. *The American Journal of Science*, 244(11), p. 772-791.

Judd, A.G., Hovland, M., 2007. Seabed Fluid Flow: the Impact on Geology, Biology and the Marine Environment. Cambridge: Cambridge UP. Print.

Karig, D.E., Peterson, N.A., Shor, G.G., 1970. Sediment-capped guyots in the Mid-Pacific Mountains. *Deep-Sea Research*, Vol. 17, p. 373-378.

Kendall, G.St.C., Schlager, W., 1981. Carbonates and relative changes in sea level. *Marine Geology*, 44, p. 181-212.

Kennet, J.P., Exon, N.F., 2004. The Cenozoic Southern Ocean: Tectonics, Sedimentation, and Climate Change Between Australia and Antartica. Washington, DC: American Geophysical Union, *Geophysical Monograph Series* 151. Print. p. 345-367.

Kenter, J.A.M., Ivanov, M., 1995. Parameters controlling acoustic properties of carbonate and volcaniclastic sediments at sites 866 and 869. *Proceedings of the Ocean Drilling Program. Scientific Results*, Vol. 143, p. 287-303.

Konishi, K., 1989. Limestone of the Daiichi Kashima Seamount and the fate of a subducting guyot: fact and speculation from the Kaiko. *Tectonophysics*, 160(1-4), p. 249-265.

Koppers, A.A.P., Duncan, R.A., Steinberger, B., 2004. Implications of a nonlinear 40Ar/39Ar age progression along the Louisville seamount trail for models of fixed and moving hot spots. *Geochem. Geophys. Geosyst*., 5, p. 1-22.

Landro, M., 1992. Modelling of GI gun signatures. *Geophysical Prospecting*, 40, p. 721-747.

Langer, M.R. and Hottinger, L., 2000. Biogeography of selected" larger" foraminifera. *Micropaleontology*, 46, p. 105-120.

Lonsdale, P., 1986. A multibeam reconnaissance of the Tonga Trench axis and its intersection with the Louisville Guyot Chain. *Marine Geophysical Researches*, 8, p. 295-327.

Lonsdale, P., 1988. Geography and History of the Louisville Hotspot Chain in the South Pacific. *Journal of Geophysical Research*, 93(B4), p. 3078-3104.

Lonsdale, P., Dieu, J. Natland, J., 1993. Posterosional Volcanism in the Cretaceous Part of the Hawaiian Hotspot Trail. *Journal of Geophysical Research*, 98(B3), p. 4081-4098.

Menard, H.W., 1984. Origin of Guyots: The Beagle to Seabeam. *Journal of Geophysical Research*, Vol. 89, No. B13, p. 11,117-11,123.

Mitchell, N.C., Lofi, J., 2008. Submarine and subaerial erosion of volcanic landscapes: comparing Pacific Ocean seamounts with Valencia Seamount, exposed during the Messinian Salinity Crisis. *Basin Research*, 20, p. 489-502.

Moore, J.G., Clague, D.A., 1992. Volcano growth and evolution of the island of Hawaii. *Geological Society of America Bulletin*, Vol. 104, p. 1471-1484.

Porter, S.C., 1972. Distribution, Morphology, and Size Frequency of Cinder Cones on Mauna Kea Volcano, Hawaii. *Geological Society of America Bulletin*, Vol. 83, p. 3607-3612.

Renema, W., 2002. Larger foraminifera as marine environmental indicators. *Scripta Geol.*, 124, p. 1-260.

Rougerie, F., Fagerstrom, J.A., 1994. Cretaceous history of Pacific Basin guyot reefs: a reappraisal based on geothermal endo-upwelling. *Paleogeography, Paleoclimatology, Paleoecology*, 112, p. 239-260.

Scarth, A., 1994. Volcanoes: An introduction. London: UCL Press Limited. Print.

Sheriff, R.E., 1975. Factors affecting seismic amplitudes. *Geophysical Prospecting*, Vol. 23, p. 125-138.

Sinton, J.M. 2009. Volcanic Islands. in Gillespie, R.G., Clague, D.A., eds. 2009. Encyclopedia of Islands. Encyclopedias of the Natural World, Vol. 2, University of California Press, p. 950-954.

Staudigel, H., Clague, D.A., 2010. The geological history of deep-sea volcanoes. *Oceanography*, 23(1), p. 58-71.

Thouret, J.C., 1999. Volcanic geomorphology- an overview. *Earth-Science Reviews*, 47, p. 95-131.

Vogt, P.R., Smoot, N.C., 1984. The Geisha Guyots: multibeam bathymetry and morphometric interpretation. *Journal of Geophysical Research*, Vol. 89, No. B13, p. 11,085-11,107.

Winterer, E.L., van Waasbergen, R., Mammerickx, J., Stuart, S., 1995. Karst morphology and diagenesis of the top of Albian limestone platforms, Mid-Pacific Mountains. *Proceedings of the Ocean Drilling Program. Scientific Results*, Vol. 143, p. 433-470.

Winterer, E.L., 1998. Cretaceous karst guyots: New evidence for the inheritance of atoll morphology from subaerial erosional terrain. *Geology*, Vol. 26, No. 1, p. 59-62.

Worthington, T., Stoffers, P., Hekinian, R., Ackermand, D., Bigalke, N., Timm, C., Unverricht, D., Zimmerer, M., 2003. Unpublished SO167 Cruise Report.